H.E. Wesseling

Influence of Current Ripple on Proton Exchange Membrane Fuel Cell Degradation

TU Delft

Influence of Current Ripple on Proton Exchange Membrane Fuel Cell Degradation

By

H.E. Wesseling

Master Thesis

in partial fulfilment of the requirements for the degree of

Master of Science
in Mechanical Engineering

at the Department Maritime and Transport Technology of Faculty Mechanical, Maritime and Materials Engineering of Delft University of Technology
to be defended publicly on Monday December 13, 2021 at 13:00.

Student number:	4369130	
MSc track:	Multi-Machine Engineering	
Report number:	2021.MME.8575	
Thesis committee:	Dr. ir. H. Polinder,	TU Delft committee Chair
	Dr. ir. L. van Biert,	TU Delft committee member
	Dr. ir. J.W. Haverkort,	TU Delft committee member
	J. Bruinsma	Company Supervisor, NedStack
Date:	November 29, 2021	

TU Delft

Abstract

The ongoing transition towards sustainable energy has resulted in a large interest in alternative sources. Proton exchange membrane fuel cells (PEMFC) use hydrogen to produce energy without harmful emissions, and they can be used in a range of applications, from mobility to industrial power generation.

One hurdle that still stands between PEMFC and widespread commercial adoption is the durability. The electrodes, catalyst and membrane of the fuel cells degrade due to the reactive environment inside the fuel cell (temperature, acidity and the presence of catalysts). This is worsened by situations with dynamic loads or start-stop cycling.

Another factor that can affect the degradation of fuel cells is the interaction between the fuel cell and the power electronics it interfaces with. The power electronics are necessary to boost and stabilize the voltages from the fuel cell, but they introduce current ripple into the fuel cell. The main objective of this research is to investigate how current ripple influences fuel cell degradation. The relevance is that the desired lifetime plays a significant role during the design of fuel cell systems, and quantitative information about the relationship between current ripple and fuel cell degradation can be used in the design process of the power electronics, where trade-offs need to be made between ripple amplitude, complexity and costs.

An analysis has been made concerning current ripple in fuel cells. Two current ripple types are mentioned in literature, low frequency current ripple and high frequency current ripple. Low frequency current ripple is created by the conversion from DC to AC by a single phase inverter, it has a frequency of 100Hz or 120Hz. High frequency current ripple is caused by the high frequency switching that occurs in any power converter. The link between these current ripple types and fuel cell degradation has mainly been investigated using experiments, but only for very specific parameters, a handful of frequencies and amplitudes. There is an absence of a quantitative analysis on the effect of different current ripple shapes on PEMFC degradation.

In this report, a model is developed which predicts the degradation of the PEMFC catalyst caused by current ripple. The model consists of two sub-models. The steady state degradation model predicts the decrease of the electrochemically active surface area (ECSA) due to the average current of the current ripple. It models the influence of electrochemical dissolution, chemical dissolution and Ostwald ripening on the ECSA over time. The ripple degradation model predicts the ECSA degradation as a function of the ripple amplitude and frequency, using an electrical representation of the fuel cell and experimental degradation data. The model can be used to help in the design process of power electronics that interface with fuel cells.

Contents

List of Figures

List of Tables

Nomenclature

Abbreviations

BOP	Balance of Plant
CO	Carbon monoxide
CO_2	Carbon dioxide
ECSA	Electrochemically Active Surface Area
EEC	Equivalent Electrical Circuit
EIS	Elechemical Impedance Spectroscopy
FC	Fuel Cell
GDL	Gas Diffusion Layer
HFCR	High Frequency Current Ripple
HSO_3	Sulphonic Acid
LPG	Liquified Petroleum Gas
MEA	Membrane Electrode Assembly
MPL	Micro Porous Layer
OCV	Open Circuit Voltage
PCU	Power Conditioning Unit
PEM	Proton Exchange Membrane
PEMFC	Proton Exchange Membrane Fuel Cell
PFSA	Perfluorinated Sulfonic Acid
PRD	Particle Radius Distribution
PTFE	Polytetrafluorethylene (Teflon)
PtO	Platinum Oxide
PWM	Pulse Width Modulation
RH	Relative Humidity
RLC	Resistor Inductor Capacitor

List of symbols

E	Electrical potential	V
$\bar{g}_f$	Gibbs free energy	j
F	Faraday's constant	$96484 C mol^{-1}$
$\eta_{\max}$	Maximum efficiency	%
$\bar{h}_f$	Molar enthalpy of formation	j
η_{HHV}	Fuel cell efficiency with regard to the higher heating value	%
V	Fuel cell voltage	V
μ_f	Fraction of hyrdogen used	
Δi_L	Current ripple peak-to-peak	A
D	Duty cycle	
V_o	Output voltage	V
L_f	Inductance	H
v_{ac}	Instantaneous AC voltage	V
V_{peak}	Peak AC voltage	$\sqrt{(2)} * 230V$
t	Time	s
i_{ac}	Instantaneous AC current	A
I_{peak}	Peak AC current	A
ω	Angular frequency	$\text{rad} s^{-1}$
ϕ	Phase shift	rad
i_{fc}^*	Instantaneous fuel cell current	A
$\Delta V_{\max}$	Maximum peak-to-peak voltage ripple	V
C	Capacitance	F
T_s	Switching period	s
R_{ct}	Activation resistance	Ω
$R_{\text{ct}}(A)$	Activation resistance at the anode	Ω
$R_{\text{ct}}(C)$	Activation resistance at the cathode	Ω
C_{dl}	Double layer capacitance	F
P_{ripple}	Power loss due to ripple	W
Z	Impedance	Ω
I_{ripple}^2	RMS of current ripple	A
I_{avg}	Average current	A
$I_{\text{amplitude}}$	Current ripple amplitude	A
V_{avg}	Average voltage	V
$n_{i,j}$	Number of platinum atoms in particle i at time step j	
$m_{i,j}$	Number of platinum oxide molecules in particle i at time step j	
Δt	Time step	s
$r_{i,j}$	Radius of particle i at time step j	m
v_1	Reaction speed of electrochemical dissolution	s^{-1}
v_2	Reaction speed of oxidation of Pt	s^{-1}
v_3	Reaction speed of dissolution of PtO	s^{-1}
v_4	Reaction speed of Ostwald ripening	s^{-1}
θ	Fraction of PtO coverage of the particle	

E_1	Equilibrium potential of electrochemical dissolution	V
E_2	Equilibrium potential of chemical dissolution	V
E_1^{∞}	Equilibrium potential of electrochemical dissolution of Pt	$1.188V$
E_2^{∞}	Equilibrium potential of oxidation of bulk Pt	$0.98V$
k_1	Reaction constant of electrochemical dissolution	s^{-1}
k_2	Reaction constant of oxidation of Pt	s^{-1}
k_3	Reaction constant of dissolution of PtO	s^{-1}
k_1^{∞}	Equilibrium rate constant of electrochemical dissolution	s^{-1}
k_2^{∞}	Equilibrium rate constant of oxidation of Pt	s^{-1}
k_3^{∞}	Equilibrium rate constant of dissolution of PtO	s^{-1}
$c_{\mathrm{H+}}$	Concentration of H^+	$MolL^{-1}$
$c_{\mathrm{H+}}^{\mathrm{ref}}$	Reference concentration of H^+	$MolL^{-1}$
R	Ideal gas constant	$8.314Jmol^{-1}K^{-1}$
T	Temperature	°C
β	Proportional constant between 0 and 1.	
γ	Interfacial surface tension	jm^{-2}
V_{Pt}	Molar volume of Pt	$9.09e-6m^3mol^{-1}$
D_m	Diffusion coefficient of Pt	m^2s^{-1}
C_{Pt}	Solubility of Pt	$10^{-6}MolL^{-1}$
l_c	Capillary length	m
$\bar{r}$	Average particle radius	m
E_{th}	Theoretical fuel cell potential	V
E^0	Standard fuel cell potential at normal conditions	V
P_{H_2}	Partial pressure of hydrogen	bar
P_{O_2}	Partial pressure of oxygen	bar
V_{cell}	Fuel cell voltage	V
$\Delta V_{\mathrm{activation}}$	Activation losses overvoltage	V
α	Charge transfer coefficient	
ΔV_{ohm}	Conduction losses overvoltage	V
β_*	Tuning parameter	
$\Delta V_{\mathrm{transport}}$	Transport losses overvoltage	V
I	Current	A
I_0	Exchange current density	A
I_{lim}	Maximum fuel cell current	A
R_{mem}	Membrane resistance	Ω
R_{act}	Activation resistance	Ω
l	Membrane thickness	cm
σS	Membrane surface area	cm^2
σ	Membrane conductivity	$\Omega^{-1}cm^{-1}$
λ_m	Membrane hydration level	
C_{dl}	Double layer capacitance	F
f_{ripple}	Ripple frequency	Hz
$ECSA_t$	Current ECSA	m^2
$ECSA_0$	Starting ECSA	m^2

1 Introduction

Many years have passed since Sir William Grove demonstrated the principle of a fuel cell in 1839 [1]. Because of its potential to be an incredible power source, efficient and clean, research and development of has been ongoing since. Unfortunately the technology has taken a long time to fulfill its promises. It took until the 1960's for fuel cells to be used in an impactful application in the NASA Gemini spacecraft program [1]. Afterwards, the development of the technology continued but it did not reach a significant level of adaption. In the twenty-first century the concern for climate change and the environment in general led to increased attention for all power sources that could be an alternative for polluting conventional fossil fuel based ones. Fuel cells produce electricity when fed with hydrogen and oxygen, while the only product is water. Its total lack of emissions make it a great power source for the transition towards sustainable energy.

The increase in attention has lead to many new applications of fuel cells. They can be used for commercial, industrial or residential power generation. In remote (off-grid) locations fuel cells can function as the primary power source or in conjunction with other renewable power sources (solar panels or wind turbines for example). The efficiency of fuel cell systems can be increased if the heat from the system can also be used (for houses or industrial processes), using combined heat and power (CHP) fuel cell systems. A related application is the use of fuel cells as a back up power source, for uninterruptible power supplies.

Fuel cell powered cars are a more complicated subject, they have to compete with battery powered electric vehicles. An additional problem is the lack of fuel-delivery. There are however fuel cell powered cars available, the Honda Clarity and the Toyota Mirai are two examples [2, 3]. There are also pilot projects with fuel cell powered buses currently in progress. Sixty four fuel cell transit buses are in active operation in the United States [4]. In the EU the JIVE and JIVE 2 projects should result in nearly 300 fuel cell buses operating all over Europe. While the projects are still ongoing, buses are already in operation [5]. Another possible transportation implementation area for fuel cells are ships. An example is the tour boat Nemo H_2, which was built to be used in Amsterdam [6].

Between all the different fuel cell variants, the proton exchange membrane fuel cell (PEMFC) is the most practical choice in a lot of cases. It trades in some performance

for a smaller and lighter implementation and can handle dynamic loads reasonably well. A problem that remains is the durability of PEMFC. Due to the reactive environment inside a fuel cell, its components degrade over time. This process is worsened by dynamic loads. A very specific dynamic load is current ripple, which is caused by the power converters that are a part of every FC system. While there are methods to reduce current ripple, they come with downsides, one of which is increased costs.

Therefore, it is important to investigate the interaction between a power converter and a fuel cell to help making design choices for FC implementations. If the interactions between the fuel cell, power electronics and the load affect the lifespan of the fuel cell significantly, it could definitely be worth it to implement more sophisticated power electronics. On the other hand, simpler (and cheaper) power electronics could be used if fuel cells are resistant to the high frequency disturbances. This leads to the following research question for the literature study:

What is the influence of current ripple introduced by power electronics on the degradation of a proton exchange membrane fuel cell?

The research question is accompanied by the following sub-questions:

- *How do proton exchange fuel cells degrade?*
- *How is the current ripple created?*
- *What are the characteristics of the current ripple?*
- *What influence does current ripple have on the performance of a fuel cell?*
- *What influence does current ripple have on the components of a fuel cell?*

The literature study revealed two research gaps, as described in 6. The first research gap is the lack of a quantitative analysis of the effect of current ripple on proton exchange membrane fuel cell degradation. The research that has been performed is often done using a specific ripple frequency, ripple amplitude and current density. Because current ripple can can occur in many shapes or forms, an indication of the FC degradation associated with a certain current ripple would be very valuable for the design of the power electronics. The second research gap is the absence of a degradation mechanism for high frequency current ripple. The influence of high frequency current ripple on fuel cells is still unclear, some research indicates it accelerates degradation, but a degradation mechanism has not even been proposed.

1.1. Research Objective

With the research gaps in mind, it is possible to establish a suitable direction for novel research. The research will aim to increase the knowledge of the influence that current ripple has on the internal components and processes of a proton exchange membrane fuel cell.

When considering the subject for new research into the impact of current ripple on fuel cells, it should be noted that while low frequency current ripple arguably has the largest influence on fuel cell degradation, focusing on just the low frequency current

ripple has a limited relevance for many applications. It requires a single phase AC-inverter to be present in the system, but conversion to three phase AC is more suitable for most grid connected fuel cell implementations. Therefore this research will not be the limited to a specific current ripple frequency, but take the whole range of possible ripple frequencies into account.

A model will be built to approximate the degradation of a PEMFC due to current ripple. This model will take the degradation of one fuel cell component into account, the catalyst. Catalyst degradation is good candidate for ripple induced decay. It is known that potential fluctuations accelerate catalyst degradation, and current ripple causes exactly that. Meanwhile the degradation mechanisms associated with the carbon electrode and the membrane are much harder to link to current ripple. Because the exact degradation mechanism for degradation of the catalyst by current ripple is unclear, experimental data is needed to base the model on.

This leads to the following research objective:

Develop a model of the current ripple induced catalyst degradation in a proton exchange membrane fuel cell.

This objective is accompanied by two sub-questions:

- *What is the impact of degradation due to current ripple compared to steady state FC degradation?*
- *How can limited experimental catalyst degradation data be extrapolated to other ripple shapes?*

The model will be build up out of two parts. The first sub-model concerns the catalyst degradation that occurs when a fuel cell is subjected to a stable DC load. Fuel cells degrade continually when under load, and it is interesting to compare the contribution of the stable load and the current ripple to the total catalyst degradation because they are both degradation sources that are 'active' during most of the lifetime of the fuel cell.

The second module models the catalyst degradation due to current ripple. This sub-model will be based on fuel cell degradation experiments performed in a lab. It will take into account the working time, ripple frequency and ripple amplitude, and predict the catalyst degradation.

1.2. Thesis structure

This thesis functions as a graduation project on the degradation of proton exchange membrane fuel cells due to current ripple. The project is a collaboration between the Delft University of Technology and NedStack Fuel Cell Technology. It aims to further the understanding of the impact of current ripple on fuel cells. Part I is the literature study, consisting of chapters 2 to 6. Chapter 2 describes the working principles of a fuel cell and its components. Chapter 3 discusses what is necessary to implement fuel cells in real world applications. Chapter 4 discusses the degradation mechanisms of the different fuel cell components. Chapter 5 introduces the concept of current ripple, its sources and its influence on a fuel cell. Chapter 6 gives a conclusion of the relevant literature and provides the directions for the follow-up research.

Part II consists of chapters 7 to 11, describing the follow-up research. Chapter 7 briefly discusses fuel cell modeling techniques and describes the structure of the model. Chapter 8 describes the methodology of modeling the catalyst degradation when the fuel cell is under a constant load. Chapter 9 describes the ripple degradation model, which calculates the catalyst damage based on the ripple shape. Chapter 10 shows the results of the combined models and describes an experiment that should be performed to be able fully utilize the model. Chapter 11 provides the conclusion and recommendations.

I

Literature review

2

Fuel cell principles

This chapter describes the basic principles of fuel cells in general. The building blocks and behavior of proton exchange membrane fuel cells are also discussed.

A fuel cell is operated by feeding it hydrogen and oxygen, the fuel cell then produces electrical energy and water. This overall reaction consists of two half-reactions, (2.1) and (2.2). In an acidic fuel call the hydrogen gas is ionized at the anode, splitting each hydrogen molecule in two protons (H^+) and two electrons, as seen in (2.1). At the cathode, (2.2), the oxygen reacts with four protons and four electrons (produced at the anode), the result of the reaction is water.

$$2H_2 \rightarrow 4H^+ + 4e^- \quad \text{(anode)} \tag{2.1}$$

$$O_2 + 4e^- + 4H^+ \rightarrow 2H_2O \quad \text{(cathode)} \tag{2.2}$$

2.1. Fuel cell types

One of the most popular variants of fuel cells is the Proton Exchange Membrane Fuel Cell, often referred to as PEM or PEMFC (and also referred to as polymer electrolyte membrane). The basic components of a PEMFC are two electrodes with an electrolyte between them. The electrolyte is a solid polymer membrane which is permeable for protons (hence the name of the fuel cell). As mentioned before, the protons that are produced at anode (2.1) need to be transported to the cathode for (2.2). But the hydrogen and oxygen need to stay separated, otherwise the fuel cell would not produce electrical energy, only heat and water. The membrane fulfills this task, only protons can pass through it, while it is impermeable for the hydrogen and oxygen.

The membranes in PEM fuel cells have been made of Nafion since it was invented in 1967 by Dupont. [1] The electrodes are made of graphite, because of its good electrical conduction and its electrochemical stability. To increase the reaction surface and to enable the diffusion of the gasses the electrodes have a porous structure. A catalyst is necessary to accelerate the reactions at both the anode and cathode. In both cases platinum is used as the catalyst, the platinum is attached to the electrodes as very small particles to maximize the reactive surface.

Fuel cell type	Mobile ion	Electrolyte	Temperature
Alkaline (AFC)	OH^-	Alkaline solution	50 - 200°C
Proton Exchange Membrane (PEMFC)	H^+	Membrane	30 - 100°C
Direct methanol (DMFC)	H^+	Membrane	20 - 90°C
Phosphoric acid (PAFC)	H^+	Phosphoric acid	~200°C
Molten carbonate (MCFC)	CO_3^{2-}	$LiOAlO_2$	~650°C
Solid oxide (SOFC)	O^{2-}	ceramic material	500 - 1000°C

Table 2.1: Comparison between different types of fuel cells [1]

Other than PEMFC there are many more types of fuel cells, with different electrolytes, mobile ions and operating temperatures. Six of the most common variants can be found in Table 2.1.

When compared to the other types of fuel cells, PEMFC has some advantages: it has a high power to weight and also a high power to volume ratio, it is also cold start capable. These characteristics are nice to have in any case, but are vital when choosing a power source for a vehicle. In a vehicle, the space is limited and extra weight requires a stronger power source. Additionally, vehicles are likely to be shut down and started up again relatively often, making the cold start capability very practical.

One of the downsides of PEMFC is that the low operating temperature limits the reaction rates of the reactions at the anode and the cathode. As mentioned before, this is counteracted by using platinum as a catalyst. The other fundamental problem is that fairly pure hydrogen is needed for operation (contaminants such as CO can damage the fuel cell), which is not readily available and can be difficult to handle.

2.2. PEMFC membrane

The membrane is arguably the most important part of the PEMFC. The task of the membrane is to keep the gasses from the anode and the cathode separated, while allowing protons to move through the electrolyte. The industry standard for proton exchange membranes is Nafion, developed and produced by Dupont [1]. The thickness of the membranes in PEMFC's depend on the balance between the resistance against proton travel and the ability to block the oxygen and hydrogen. A thicker membrane lets less hydrogen pass through, while a thinner membrane leads to less resistance for the protons. PEMFC membranes have a thickness of around 100 µm [7].

The foundation of the membrane is polyethylene, a very basic polymer. Polyethylene, the molecular structure of which can be seen in Figure 2.1b, is a long chain of carbon atoms surrounded by hydrogen. It is produced by polymerizing ethylene (Figure 2.1a).

The hydrogen atoms from the polyethylene are then substituted for fluorine, in a process called perfluorination. The resulting molecule is polytetrafluoroethylene, or PTFE for short. The molecular stucture of PTFE can be seen in Figure 2.2. PTFE is more commonly known as Teflon, a material with a number of very useful properties such as chemical inertness, heat resistance, hydrophobicity and a low coefficient of friction. This PTFE polymer is then 'sulphonated', as side chains are added with sulfo group (HSO_3) at the end. This gives the final material, perfluorinated sulfonic acid

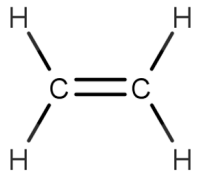

(a) Structure of Ethylene

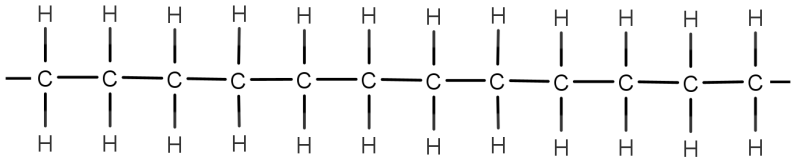

(b) Structure of polyethylene

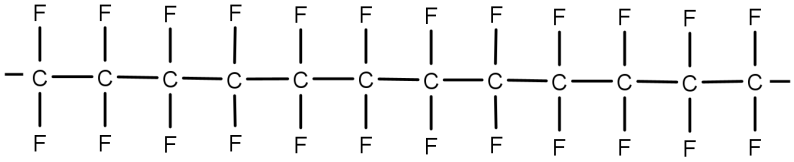

Figure 2.2: Structure of PTFE

(PFSA), the molecular structure of which can be seen in Figure 2.3 [8]. The HSO_3 group at the end is ionically bonded, which means that the H^+ is not securely attached to the side chain, it is only attracted to it. The charged side chains make the whole molecule an ionomer, a polymer with multiple ionized units attached to the backbone. The presence of the HSO_3 groups and the protons influence the behavior of the material. The oppositely charged ions attract each other, forming clusters of sidechains in the structure of the material [1]. The sulphonic acid groups are hydrophilic, while the rest of the material is hydrophobic (because it is practically PTFE). This gives the membrane the ability to absorb water at those clusters of side chains. Protons can move easily through the hydrated regions and hop from cluster to cluster to travel across the membrane. To let the protons travel easily through the membrane it is important to keep the membrane well hydrated.

2.3. PEMFC Electrodes

The PEMFC electrodes are primarily made of carbon and have multiple important roles.

- It is the support for the catalyst
- It makes the electrical connection between the catalyst and the outside world
- It helps in the distribution of the gasses through the fuel cell
- It carries water away from the membrane surface

To fulfill all these tasks a PEMFC electrode consists of multiple structures [9]. A distinction that is often made is between the active layer (or catalytic layer) and the gas diffusion layer (GDL). The active layer is the part of the electrode that is in contact with the electrolyte. On the active layer, the platinum (the catalyst) is attached to the carbon support in the form of very small particles (nanometer-scale). This is done to maximize the available surface area for the reactions. Less than 0.5 mg/cm^{-2} of

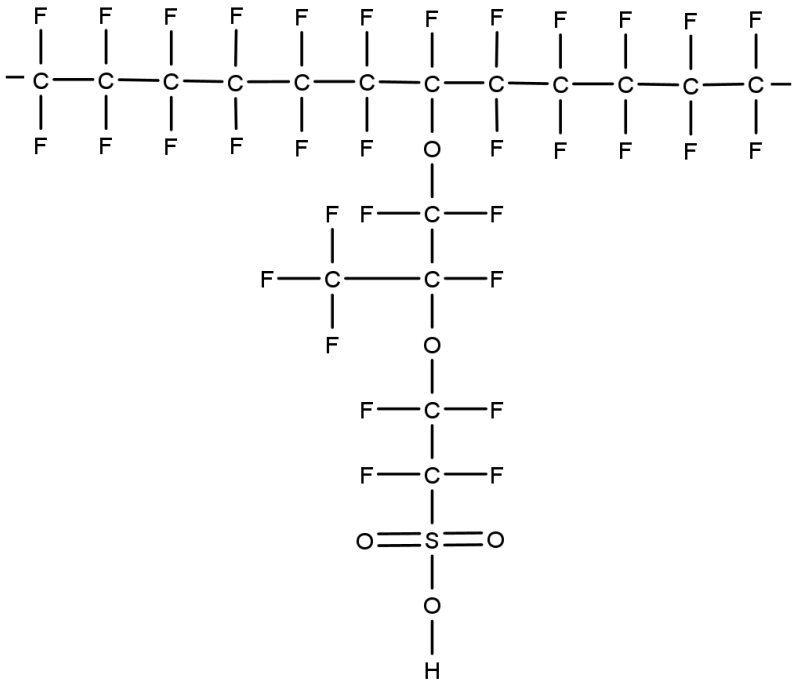

Figure 2.3: Structure of sulphonated fluoroethylene

platinum is used in modern fuel cells [1, 9]. The electrode itself is made of a powder in this layer. This gives a microporous structure which helps the distribution of the gasses to the platinum particles. An example of a powder that is used in PEMFC is XC72 (®Cabot)[1], XC72 is advertised as having a particle size smaller than 44 micron[10]. For reference, particles of 44 micron are very small, but they are around 100,000 times larger than the platinum particles.

The gas diffusion layer also has a porous structure to promote the transport of gasses and water, but on a different scale. In that context it is sometimes referred to as the macroporous layer. This layer is made out of carbon paper or carbon cloth [1]. PTFE is added to the gas diffusion layer (and sometimes the active layer) to help move water away from the catalyst.

2.4. Water management

The hydration level of the membrane in the fuel cell needs to be carefully controlled. As mentioned in Subsection 2.2, the proton conductivity of the membrane strongly depends on the hydration level. Insufficient hydration could even permanently damage the membrane [11]. A second water management task is the removal of water from the cathode. The reaction at the cathode produces water which needs to be removed from the catalyst layer as quickly as possible to prevent a build up of water that would block the reactants from accessing the reaction sites. An important phenomenon related to the water management is electro-osmotic drag, every proton that travels trough the membrane pulls multiple water molecules (between 1 and 5 [1]) along with them out of the membrane to the cathode. Electro-osmotic drag thus contributes to both the dehydration of the membrane and to the flooding of the cathode.

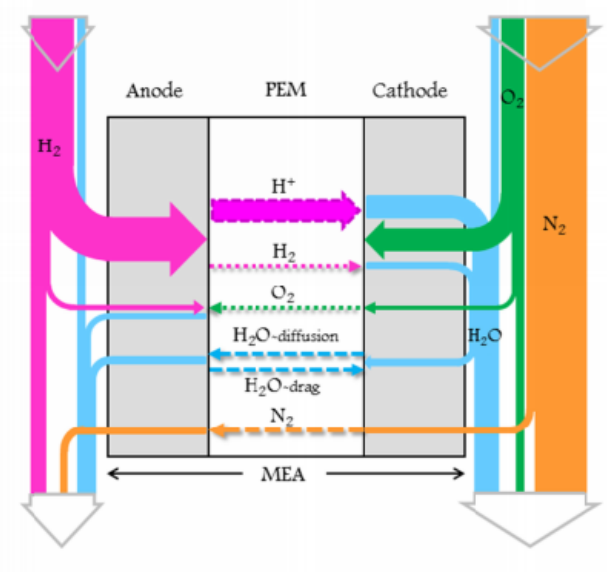

Figure 2.4: Flows of gasses and liquids inside a PEMFC [11]

Both the hydration level of the membrane and the cathode water removal are influenced by the relative humidity of the air that is fed into the fuel cell. The relative humidity of the air needs to be between 80% and 100%. When the humidity is too low, the air dries out the membrane. When the humidity is to high, liquid water can collect in the electrodes, preventing the gasses from being transported properly or inhibiting the reactions themselves at the catalysts. It can also be necessary to humidify the hydrogen inlet to also humidify the membrane from the anode side.

2.5. Reactant management

In a PEMFC the reactants are fed into the cell in a gaseous state, on the anode side hydrogen and on the cathode side (filtered) air. They should remain at their respective electrode, but as can be seen in Figure 2.4, there are multiple gasses flowing through the membrane.

On both sides more reactants are fed into the cell than necessary for the reactions, i.e. a stoichiometry (λ) of more than 1. This is done to make sure that there is always enough reactants at the platinum particles, to limit the so called concentration losses. The higher larger amount of air also helps with the removal of water from the cell.

While using more air is not a problem, since it is freely available everywhere, just pumping extra hydrogen into the fuel cell that is not going to be used for energy production, is not acceptable. Therefore the excess hydrogen is recirculated, it is added to the new hydrogen at the inlet. That way, no hydrogen is wasted.

The membrane is not perfect, there is always a small amount of H_2 that crosses to the cathode, and O_2 and N_2 that crosses over to the anode. This worsens when the cell starts to age. For the reactants it is obvious that crossover is harmful for the performance of the fuel cell, when they are at the wrong side of the membrane, they can't contribute to electricity-creating reactions. The nitrogen can also cause complications. Because of the recirculation of the hydrogen (and thus the recirculation

of nitrogen) the initially small nitrogen fraction can grow until it can hinder the hydrogen from reaching all the catalyst.

This can be solved through 'breaking' the recirculation by bleeding or purging the hydrogen. Bleeding is removing a part of the gasses from the anode outlet (1% - 5% [11]). Purging is periodically removing a significant part of the gasses at the anode outlet. It should be noted that the nitrogen crossover increases when the membrane ages, which means that the bleeding fraction or the purging frequency should change over the lifetime of the fuel cell.

2.6. Theoretical voltage of PEMFC

A fuel cell can produce electricity because of the electrical potential difference between the reaction that take place at the anode and the cathode. This potential difference, or the reversible open circuit voltage (OCV), can be calculated using the Gibbs free energy released and the Faraday constant. The Gibbs free energy is: *'energy available to do external work, neglecting any work done by changes in pressure and/or volume'* [1]. When the Gibbs free energy of the reaction products is subtracted from the Gibbs free energy of the reactants, the result is the Gibbs free energy released ($\bar{g}_f$)(in this case per mole for convenience).

The reversible OCV can be obtained by dividing the energy by the charge that flows between the electrodes. As mentioned before, for every hydrogen molecule, two electrons are produced, which gives a charge of -2F coulombs per mole of hydrogen. F is Faraday's constant, the charge of one mole of electrons. This leads to (2.3), where $\bar{g}_f$ is the Gibbs free energy released and F is Faraday's constant.

$$E = \frac{-\Delta \bar{g}_f}{2F} \tag{2.3}$$

The Gibbs free energy is dependent on the temperature and state of the agents (liquid or gaseous). For example, a PEMFC operating at 80°C has an reversible OCV of 1.17V.

The theoretical maximum efficiency of a fuel cell is given by (2.4), where $\bar{h}_f$ is the molar enthalpy of formation.

$$\eta_{\text{max}} = \frac{\Delta \bar{g}_f}{\Delta \bar{h}_f} * 100 \tag{2.4}$$

This can be simplified for hydrogen fuel cells into (2.5). Detailing the efficiency associated to the higher heating value, where V is the voltage of the fuel cell and μ_f is the fraction of the hydrogen that is actually consumed (for an explanation of why not 100% of the hydrogen is used, see Section 2.5).

$$\eta_{\text{HHV}} = \mu_f \frac{V}{1.48} * 100 \tag{2.5}$$

2.7. Polarization losses

The reversible open circuit voltage is the theoretical maximum voltage of a fuel cell, without a load (this is where the name open circuit voltage comes from, there is no closed electrical circuit). In the real world, this voltage level is never reached, due tot

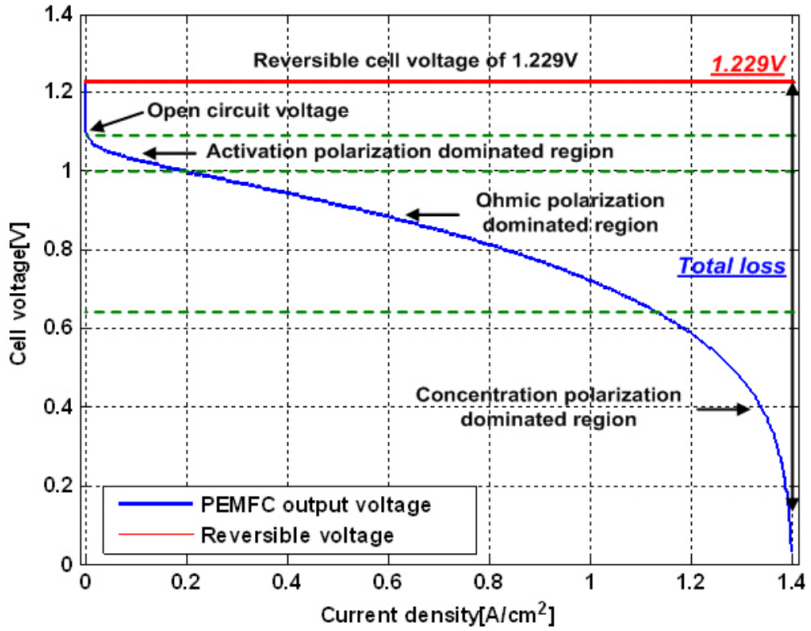

Figure 2.5: A schematic polarization curve of a PEMFC [12].

a number of factors. These voltage losses are referred to by a number of different names, originating in all the engineering fields that fuel cell technology applies to. Terms used in literature are: polarization, overvoltage, overpotential, irreversibility, voltage drop or just the general 'loss'.

An interesting characteristic of a Fuel cell is its voltage plotted against the current density, this is done in the polarization curve. A typical PEMFC polarization curve can be seen in Figure 2.5

There are three important sources of polarization: activation losses, conduction losses and concentration losses.

2.7.1. Activation losses

The reactions in the fuel cell only start occurring when their respective activation energies are overcome. This is reflected as a steep voltage drop at the start of the polarization curve. An additional voltage drop is caused by the electrons having to travel into and out of the electrodes [11]. The reaction at the anode is much faster than the reaction at the cathode. When considering the activation losses of a PEMFC the contribution of the cathode can generally be neglected [1].

There are several ways to reduce the activation losses. Raising the temperature is the simplest way, but not feasible for PEMFC's. The membrane needs liquid water, making it difficult to raise the temperature above 100°C. This limitation make the activation losses a bigger issue for PEMFC than for other fuel cell variants. The platinum catalyst is used in PEMFC to overcome this handicap. More catalyst (surface area) reduces the activation losses. Increasing the pressure also helps the reactions.[1, 11]

2.7.2. Conduction losses

There are two sources of conduction losses. The electrical resistance of the electrodes, and the resistance of the electrolyte to the flow of protons. The conduction losses follow Ohms law and are responsible for the straight part halfway the polarization curve. There is little that can be done to influence the conduction losses, they depend mainly on the thickness of the membrane and the material of the electrodes.

2.7.3. Concentration losses

For the reactions to occur the reactant(s) need to be present at the catalyst. The reactions products then have to be removed to make space for the next molecules to react. At higher current densities more reactant needs to be supplied to the catalyst particles and more reaction product needs to be removed. There is a limit to the transport capabilities of the GDL and the active layer. When the reactants are consumed faster that they are supplied, or when the products are collecting on the platinum particles, the fuel cell voltage will drop. The concentration losses only influence the fuel cell voltage at high current densities, therefore they can be seen at the end of the polarization curve, as a downwards slope.

2.7.4. Fuel crossover

Fuel crossover, when hydrogen passes through the membrane, is another polarization source. But in contrast with the aforementioned three, it has a negligible effect during operation [1]. Fuel crossover does however have a notable influence on the OCV. Even if there is no closed circuit, the hydrogen diffuses through the membrane and when it reaches the cathode, it reacts with the oxygen that is present there. Because of that, the activation losses come into play, lowering the open cell voltage.

2.8. Conclusion

In this chapter, the working principle of the proton exchange membrane fuel cell have been explained. It converts hydrogen and oxygen into electricity through two half reactions occurring at their respective electrode. The electrodes are made of carbon, with platinum particles to catalyze the reactions, the electrolyte is a polymer membrane that is permeable for protons. The voltage at which PEMFC function is affected by multiple irreversibilities: activation-, conduction-, concentration losses and fuel crossover.

3

Implementation of fuel cells

This chapter explains what is needed to implement a fuel cell system.

To get from a single fuel cell in a lab to an energy source that is usable in the real world, a lot more engineering work is required. The reactants need to be supplied to the fuel cells (at specific conditions), while the water and excess air need to be removed. The temperature needs to stay within the operating limits, and the characteristics of the generated power should meet the requirements of the associated load. And everything needs to be monitored and controlled closely.

3.1. PEMFC Stack

While a fuel cell can deliver hundreds of amps, the voltage under load of a PEMFC is relatively low (around 0.7V). To increase the voltage to a more practical level, multiple fuel cells are stacked. The fuel cell is in this context often referred to as a membrane electrode assembly (MEA). Stacking the fuel cells introduces a number of problems with regard to reactant transport and temperature. The stacked fuel cells need to be fed from the side, but the gasses should still be distributed evenly over the surface of the cell. Additionally, the fuel cells generate heat, and when they are sandwiched in between other heat producing fuel cells they will overheat unless they are actively cooled. These problems are solved by the bipolar plate.

3.1.1. Bipolar plates

Bipolar plates are placed between the MEA's. They electrically connect the cells and are also responsible for the distribution of the reactants to the fuel cell on either side. Additionally the bipolar plates are used to cool the fuel cell stack, for that purpose there are coolant channels present in the plates. Bipolar plates can be made from graphite, metal or composite materials (corrosion resistant polymers and conductive additives)[13]. They all have their advantages and disadvantages with regard to strength, conductivity, corrosion resistance, costs and more. A design choice that has to be made for bipolar plates is the flow field pattern, which determines how the gasses are distributed over the fuel cell surface. There are two basic flow field patterns. Firstly there are the parallel systems, with multiple parallel grooves distributing the reactants. An example can be seen in Figure 3.1a. The main drawback of this

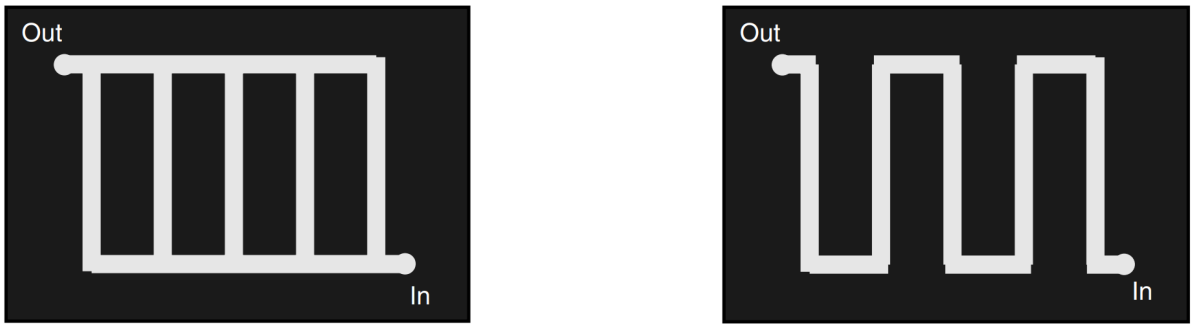

(a) Parallel flow field

(b) Serpentine flow field

Figure 3.1: Basic flow field patterns for bipolar plates

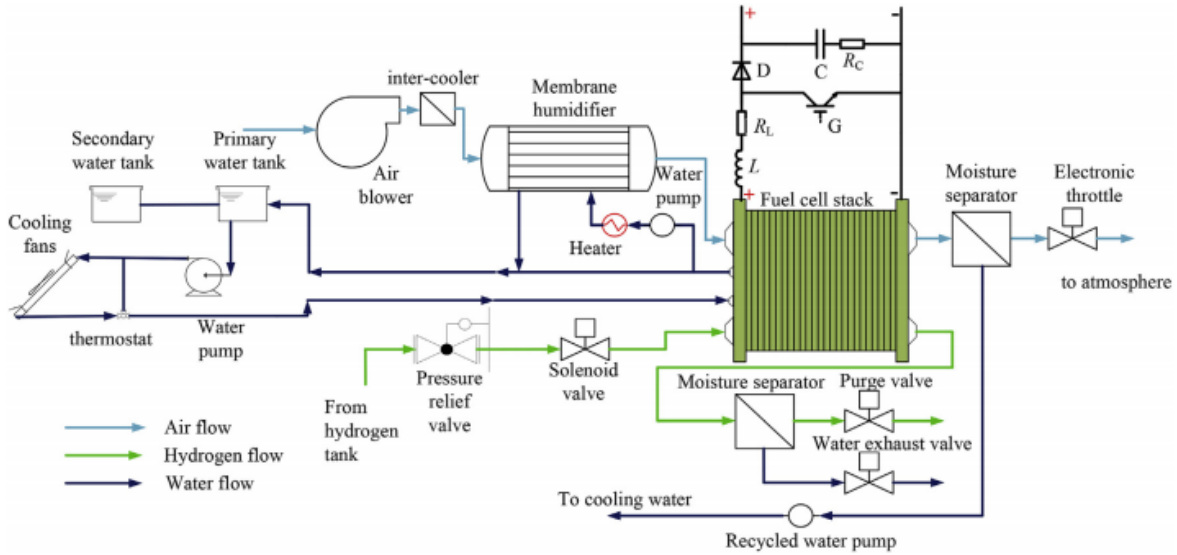

Figure 3.2: Auxilliary equipment needed for a fuel stack to function [14]

system is that it is possible for water or nitrogen to build up in one of the channels. The second flow field pattern does not have this problem, the serpentine pattern consists of a single channel that snakes around, see Figure 3.1b. Any build up will get pushed out of the system. However, this does mean that more work has to be done to push the gasses through the bipolar plate. These two patterns can also be combined in countless ways to find the best balance between these problems.

3.2. Balance of plant

Most of the volume and weight of a fuel cell system is taken up by the balance of plant (BOP) and not by the stack itself. The BOP consists of all the equipment that is needed for the fuel cell to function. An example can be found in Figure 3.2. The main tasks of the BOP is to deliver the reactants at the correct conditions (pressure, temperature, humidity) and to cool the stack. It does this with a system of pumps, valves, a humidifier, moisture separators and more. The power electronics that convert the electricity from the fuel cell are also part of the BOP.

3.3. Hydrogen storage

Every fuel cell implementation needs a hydrogen source. Hydrogen storage comes with a unique set of problems, it has a very low energy density (energy per cubic meter). One way to increase the energy density is by storing the hydrogen under very high pressures. It also is hard to liquefy hydrogen, as can be done with LPG for example, the hydrogen would need to be cooled to 22K. The most straightforward hydrogen storage is in pressurized cylinders, which is widely used [1]. More complex storage methods bind the hydrogen to certain metals or carbon nano structures. Another option is using a substances whose molecules contain hydrogen atoms, methane, methanol or ammonia for example. In these cases the hydrogen needs to be extracted before it can be used, which requires extra equipment, increasing the size, weight and cost of the system.

3.4. Power electronics

The voltage of a fuel cell is low and unregulated (see Figure 2.5), it needs to be boosted and stabilized (a constant voltage for the whole power range) to be useful.

As mentioned before, fuel cells are stacked to deliver higher voltages. One could simply stack fuel cells until the voltage is close to the required level, but more fuel cells increases the complexity of the balance of plant systems. Therefore, the stacking is usually limited to around 100 cells [15] leading to a voltage of under 100 V. In many applications (transport or 230V AC-grid for example) this is still too low. Therefore power electronics are necessary (also referred to as power conditioning units (PCU)) to keep the voltages and currents within the limits that are necessary for the load to function correctly.

There are a lot of possible applications for fuel cells, vehicles, ships, off-grid power generation, back-up power for hospitals etc. All of these applications have different power demands. But there are also other characteristics such as high power transients or the ability to store energy that is delivered to the power system (for example in case of regenerative braking for cars). To obtain these results it can even be necessary to add extra power sources to the system, such as batteries or super capacitors. Additionally, a DC-AC conversion could be necessary (e.g. applications attached to the grid), or the isolation of inputs and outputs (for safety reasons).

All these different applications give different requirements for the associated power electronics, and therefore, there is a multitude of possible power electronics systems configurations for fuel cells. Some general preferred characteristics for power converters in FC systems are [16]:

- High efficiency
- High power density
- Small size and light weight
- Low electromagnetic interference
- Low current ripple
- Low cost

3.5. Conclusion

This chapter describes the environment in which PEM fuel cells function. A fuel cell cannot operate without a number of supporting systems. A fuel cell performs best when there are sufficient reactants and they are spread evenly across the electrode surface and the membrane is fully hydrated. These internal conditions are dependent on the delivery of the gasses to the fuel cell, the flow rate, pressure, temperature and relative humidity need to be within certain limits. On the other side of the fuel cell, the voltage of the fuel cell needs to be stabilized and boosted. Power electronics are responsible for converting the power from the fuel cell to have the needed characteristics. All the systems that interface with a fuel cell can affect the behavior of the cell, the performance or efficiency, in the worst case it can even damage the fuel cell.

4

Degradation of fuel cells

This chapter gives an overview of the ways a fuel cell degrades when in operation, this is important because the degradation that is caused by current ripple will most likely happen through one of the described degradation mechanisms.

The durability of PEMFC is a topic that gets a lot of attention because it is a field where the technology still needs to improve significantly. The US department of energy states that the durability of PEMFC is one of the main barriers for adoption in automotive applications, the other barrier being the cost [17].

The durability of a fuel cell is determined by the degradation of the individual fuel cell components. While the degradation mechanisms differ, all the basic building blocks of a fuel cell can degrade in a way that impacts the performance. It is also generally acknowledged that load transients cause significantly more degradation than static operation [18]. One part of degradation prevention can therefore be done by designing the control and power systems surrounding the fuel cell in a way that reduces or smooths out the power transients. An example is the proposal of a fuel cell powered electric vehicle by Zhang et al. [18], using a battery to keep the load on the multiple fuel cells as close to static as possible.

4.1. Catalyst degradation

The surface area of the catalyst is a very interesting parameter. Since the reactions take place on the platinum particles, more surface area means more space for reactions. This principle is embodied in the electrochemically active surface area (ECSA). To make the ECSA as large as possible with the as little (expensive) platinum as possible, the platinum is divided into very small particles.

Degradation of the catalyst is reflected in a decrease of the ECSA. The decrease is strongly associated with a transformation of the particle radius distribution (PRD) [19], this means that the platinum particles are changing in size. The radius of the platinum particles changes mainly for four reasons: dissolution, Ostwald ripening, coalescence and detaching [20]. Catalyst degradation happens at steady state operation, but is accelerated by load transients [19].

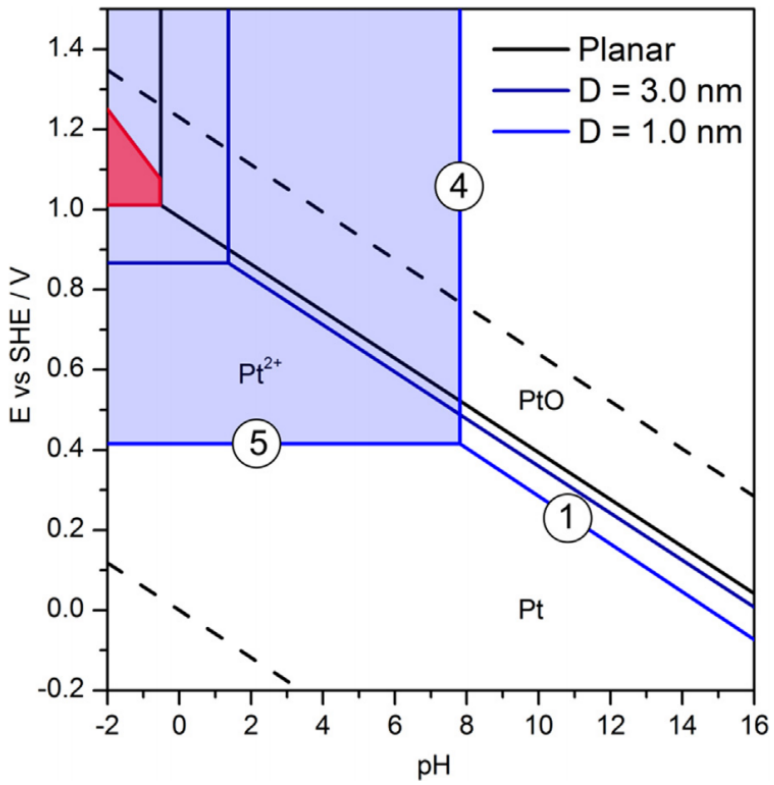

Figure 4.1: Pourbaix diagram for nanoscale platinum particles. The shaded areas represent the regions for Pt^{2+} stability for planar platinum (red) and particles with a diameter of 1 nm. The area between the dashed lines denotes the region of stability of water [22].

4.1.1. Platinum dissolution

Despite platinum being a very stable and non-reactive metal, the conditions in a PEMFC (low pH, high temperature and potential cycling) are known to promote platinum dissolution [20]. Despite the research that has been done with this subject, the exact dissolution reaction paths and products have not yet been confirmed, but the main reaction product are considered to be Pt^{2+} and PtO [19]. The dissolved platinum can then either wash away with the water that leaves the fuel cell, or be deposited in the membrane [21].

A platinum oxide layer is formed on the platinum particles under certain conditions. A Pourbaix diagram shows the stable phase of a material for the present electric potential and the pH. The Pourbaix diagram for nanoscale platinum particles can be found in Figure 4.1. For reference, the pH in a fuel cell is low, around 1, and constant. It can be seen that larger catalyst particles (>5 nm), the stable phase for platinum in a fuel cell is either Pt or PtO depending on the potential. It should be noted that the Pourbaix diagram assumes a stable situation.

The oxide layer protects the platinum particle from electrochemically dissolving, but also impedes the catalyst from doing its job. Depending on the presence (and the extent) of an oxide layer on a catalyst particle, electrochemical dissolution (4.1), or chemical dissolution (4.2) and (4.3) can take place.

$$\mathrm{Pt} \leftrightarrow \mathrm{Pt}^{2+} + 2e^{-} \tag{4.1}$$

$$\mathrm{Pt} + \mathrm{H_2O} \leftrightarrow \mathrm{PtO} + 2\mathrm{H^+} + 2e^- \tag{4.2}$$

$$\mathrm{PtO} + 2\mathrm{H^+} \leftrightarrow \mathrm{Pt^{2+}} + \mathrm{H_2O} - \tag{4.3}$$

PEM fuel cell aging experiments have made it clear that platinum dissolution is not the only reason for catalyst degradation. During these experiments, the ECSA drops quickly at first, but then stabilizes. This behavior can not be explained by just platinum dissolution with particles that just keep shrinking. What actually happens are two processes that don't influence the amount of solid platinum that is present, but that do affect the particle radius distribution.

4.1.2. Ostwald ripening

Firstly there is Ostwald ripening, a process where a large nanoparticle grows by atoms that are dissolved from smaller nanoparticles. Electrochemical Ostwald ripening is driven by the difference in electrochemical potential between particles of a different size. The bigger the particle, the smaller the chemical potential (Gibbs–Thomson energy or Ostwald–Freundlich equation). Because of difference in chemical potential, Pt^{2+} ions dissolve from the smaller particles, and precipitate on the larger particles. The difference in charge that the transferring of the ions causes, leads to electrons traveling from the smaller particles through the carbon support to the larger particles.

4.1.3. Platinum particle coalescence

A phenomenon that is in practice very similar to Ostwald ripening of platinum particles, is the coalescence of small nanoparticles into a larger one. The platinum particles can move around on the surface of the carbon support structure, they are not strongly attached to one place. If two Pt particles collide they can coalesce, and turn into one larger particle. This mechanism is most likely to be helped by liquid water in the catalyst layers. It is also suspected to be the main reason for loss of ECSA at low potentials, where Oswald ripening is negligible.

It should be noted that it is difficult to distinguish between Ostwald ripening and the coalescence of particles in experiments, since they both involve the disappearance of small particles and an increase of the number of larger particles.

4.1.4. Detaching of platinum particles

Although strictly more related to the degradation of the electrode, carbon corrosion of the support of the catalyst can lead to platinum particles detaching from the electrode. This can lead to performance degradation when the particles become isolated from the electrode or when drifting catalyst particles agglomerate. [23]

4.1.5. Influence of operating conditions on catalyst degradation

The working conditions in the fuel cell significantly influence the degradation of the catalyst. The degradation rate of the catalyst is accelerated at higher fuel cell potentials [24]. This means that, counter-intuitively, the catalyst degrades slower when the load is higher. The relation between catalyst degradation and potential also leads to more ECSA loss at the cathode than at the anode.

The relative humidity also has an impact on the catalyst degradation [24]. A (very low) relative humidity of 25% reduces the ECSA loss immensely, while 100% RH is a worst case scenario for catalyst degradation. Similarly, a higher temperature leads to faster decay [24].

Contaminants in the reactants can also damage the catalyst [25]. CO is a harmful contaminant that is likely to be present in a fuel cell in some capacity. When hydrogen is produced by reforming methane, there will some CO present in the end product. CO will adsorb onto the Pt particles and reduce the catalyst surface available.

A topic that is less well understood is the influence of load transients on catalyst degradation. It is clear that they accelerate the ECSA loss, but research has not yet yielded a definitive answer on why load transients this happens.

One partial explanation can be found in the behavior of the aforementioned oxide layer on the catalyst particles. The portion of the particles that is covered with an oxide layer depends on the electric potential. When the potential goes from high to low, the oxide layer is reduced which causes part of the platinum to be lost. Hiraoka, Matsuzawa, and Mitsushima [26] investigated whether the type of load transient influences the ECSA degradation. They found that a step up to high potential and a gradual decrease of the potential resulted in the most degradation. They speculated that the step up to a high potential resulted in more electrochemical dissolution because the formation of the oxide layer lagged behind the potential. While the gradual decrease of potential gave ample time for the reduction of the oxide layer before the potential rose again.

4.2. Electrode degradation

As mentioned in Section 2.3 the electrodes consists of two different parts, the microporous structure in the active layer and the macroporous gas diffusion layer. Both layers can be prone to degradation, but there is an important difference between the layers with regard to degradation, the presence of the catalyst in the active layer. Platinum does not only accelerate the electricity generating reactions but also harmful ones [27].

Carbon corrosion is therefore only a concern in the catalyst layer [20]. As mentioned before, carbon corrosion of the active layer can dislodge platinum particles and reduce performance. Another possibility is that the carbon corrosion changes the physical structure of the MPL, inhibiting the transport of gasses and water to and from the catalyst.

Carbon corrosion is in this case analogous to the corrosion of metal, it is the degradation of the material by oxidation. This process can be described by (4.4). This reaction is made up out of two sub reactions, firstly (4.5), where carbon at the surface is transformed into CO. And subsequently (4.6) happens, where Pt catalyses the conversion of the CO into CO_2. The CO_2 then leaves the fuel cell together with the other gasses. The first reaction seems relatively harmless, as it does not remove carbon from the electrode. But it does increase the hydrophilicity of the active layer, making it harder to remove water from the electrodes.

$$\mathrm{C} + 2\mathrm{H_2O} \leftrightarrow \mathrm{CO_2} + 4\mathrm{H^+} + 4e^- \tag{4.4}$$

$$C + H_2O \rightarrow CO_{surf} + 2H^+ + 2e^- \tag{4.5}$$

$$CO_{surf} + H_2O \xrightarrow{Pt} CO_2 + 2H^+ + 2e^- \tag{4.6}$$

While this process can occur at standard operating conditions, the reaction rates are relatively slow. The corrosion of the microporous carbon layer is mainly associated with start-stop cycling and fuel starvation [9]. Both these situations lead to a (local) lack of hydrogen.

During the start-up of a fuel cell an $O_2\backslash H_2$ front travels through the cell [28]. The presence of oxygen at the anode lowers the membrane potential which results in high cathode potentials. This enables the carbon corrosion reaction (4.4) among with the electrolysis of water at the cathode. At the anode, water is formed through (2.2). The same process happens when local hydrogen starvation occurs, because of electrode flooding or blocked transport channels. The only difference is the origin of the oxygen at the anode, in the case of (local) fuel starvation, the oxygen diffuses through the membrane from the cathode.

A final consideration about the catalyst layer is the water removal capacity. The decomposition of the PTFE binder used in the active layer decreases the hydrophobicity of the electrode. Little research has been done into this specific subject, but there is evidence that the PTFE can decompose in fuel cells. [9].

For the gas diffusion layer to be able to fulfill its task of transporting gasses and water, the porous physical structure and the hydrophobicity (PTFE coating) need to stay intact. There are multiple mechanisms for the GDL to degrade, but research into this area is still relatively limited [29].

Liquid water is present in the GDL, and some GDL components can dissolve in (acidic) water. Additionally, the flow of gas can erode the GDL. These two factors can both damage the carbon structure and degrade the PTFE. Finally there is the chemical surface oxidation of the carbon structure that can reduce the hydrophobicity of the GDL.

4.3. Membrane degradation

The degradation mechanism for the PFSA membrane can be divided into three categories: mechanical degradation, thermal degradation and chemical degradation. [9, 23] The gas separation and the proton conductivity properties of the membrane can both be impacted by degradation.

Mechanical degradation of the membrane starts even before the fuel cell ever operates. Defects from the membrane production or its inclusion into the MEA can later turn into perforations or cracks. Another factor is fatigue due to cyclic loads associated to the temperature and the hydration of the membrane (it swells and shrink depending on its water content). Mechanical degradation mainly influences the gas separation characteristics of the membrane.

Thermal degradation is negligible when a fuel cell is operating at standard conditions (~80 °C). When the temperature rises to 95 °C the ion conductivity decreases, even higher temperatures can cause more damage [20].

The main cause for the chemical degradation of the membrane is the production of H_2O_2. [23] (its unclear if this happens at the anode or the cathode or both). When the H_2O_2 breaks down, HO• and HOO• radicals are formed. These radicals then 'attack' the PFSA backbone or the sidechains. This can be diagnosed by checking the cathode outlet for fluoride, which is released when the membrane in damaged. A subject related to the chemical degradation of the membrane is the presence of foreign cations in the membrane. Foreign cations (originating from other parts of the fuel cell implementation) are more strongly attracted to the sulphate groups in the membrane, thereby hindering the transport of protons through the membrane. The degradation of the membrane can in its turn influence other (degradation) processes in the fuel cell. In Figure 4.2 an overview can be seen of membrane degradation mechanisms and their indirect consequences.

All the degradation mechanisms of the catalyst and the electrodes discussed before negatively influence the performance of the membrane, but won't lead to a total failure of the fuel cell. Severe membrane degradation can lead to the failure of a fuel cell, when the cracks and holes in the membrane grow too large, the oxygen and hydrogen can easily travel to the other side. This stops the fuel cell from producing electrical energy.

4.4. PEMFC degradation in practice

Degradation of fuel cells is a complicated topic. Even this brief overview shows that the different components have multiple degradation mechanisms and that the degradation of one component can influence other processes that are occurring in the fuel cell. Research into the degradation of PEMFC is still an ongoing process, both in the experimental and the modeling space.

What is clear, is that certain conditions are almost always detrimental to the health of a fuel cell. Start-stop-cycling, operating under OCV conditions, large load transients and lacking temperature/humidity control should be avoided to not decrease the lifetime of the fuel cell.

A side note on this topic is FC degradation because of freezing. This is mainly a concern for PEMFC's that would be applied in vehicles. When a fuel cell powererd vehicle is turned off and outside in a cold winter, it is very likely that the fuel cell itself will reach sub-zero temperatures. Because of the presence of liquid water in the membrane and the electrodes, freezing damage is a very real danger. For fuel cells in those conditions preventative measures need to be taken, such as extra isolation or heating.

4.5. Conclusion

In this chapter an overview of the degradation mechanisms of fuel cell components has been given. The catalyst, electrode, and membrane of a PEMFC all degrade over time and usage. When under normal operating conditions the catalyst is arguably the least durable, it's degradation is significantly accelerated by load transients. The degradation decreases the surface that is available for reactions (ECSA), either by dissolution of Pt or the merging of Pt particles. The carbon in the electrodes only degrades when a local lack of hydrogen at the anode enables the carbon corrosion reaction. Lo-

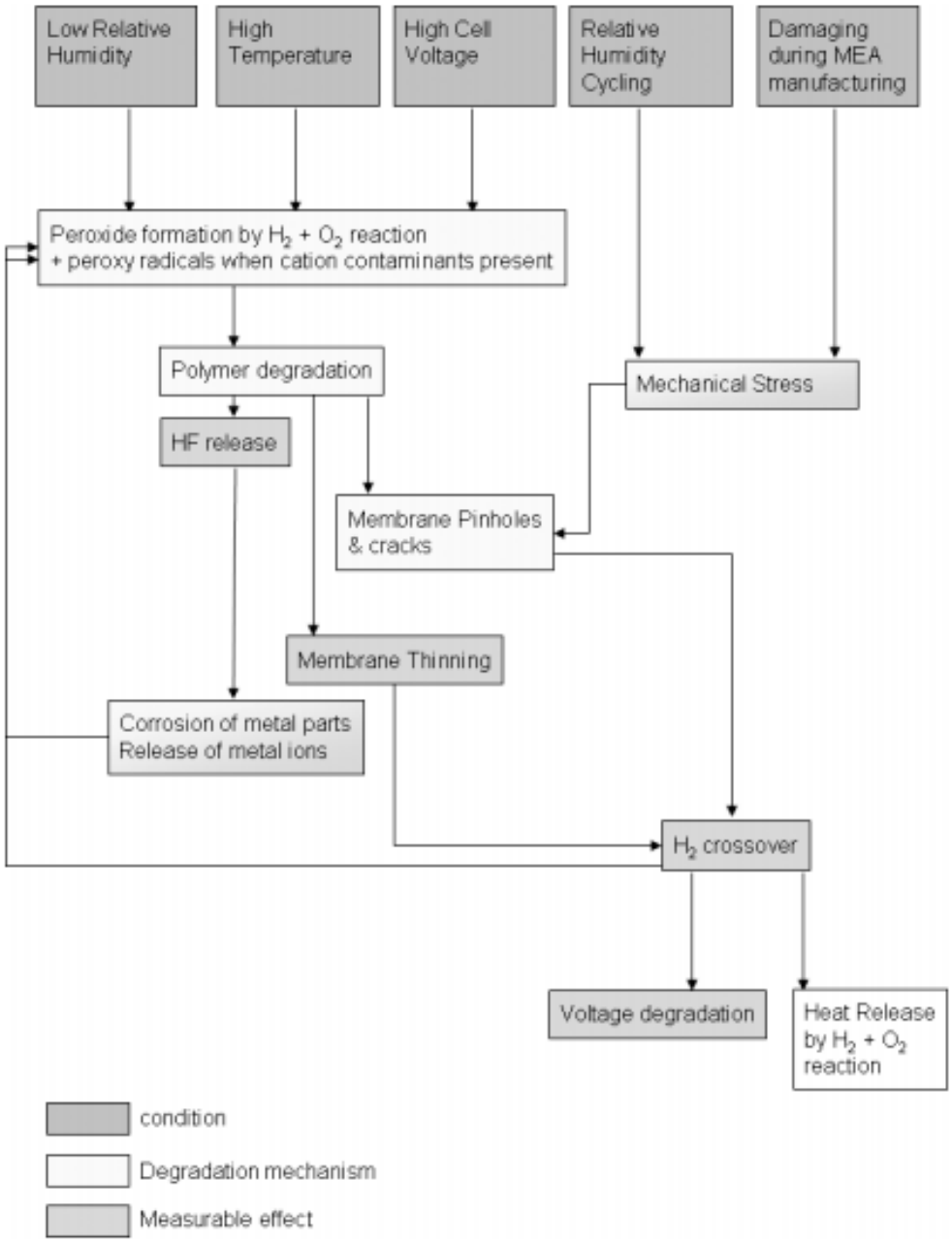

Figure 4.2: Overview of different membrane degradation mechanisms and their relations. [9]

cal fuel starvation can occur because of defects in the gas diffusion channels in the GDL or catalyst layer, or because of start-stop-cycling. Dynamic operation also has an influence on membrane degradation. The changes in water content in the membrane lead to swelling and shrinking. This results in stress cycles in the constrained membrane, and eventually cracks and pinholes due to fatigue. The membrane is also susceptible to chemical degradation, the creation and subsequent breakdown of H_2O_2 creates radicals that damage the membrane. Membrane degradation can even lead to catastrophic failure of a fuel cell, when there are too much cracks and holes in the membrane and gasses can easily pass through.

When considering the impact of current ripple on FC durability, accelerated catalyst degradation seems like the most likely option. It is known that load fluctuations accelerate ECSA degradation and disturbances in the FC current could very well have a similar effect. Carbon corrosion seems very unlikely because that is strongly linked with fuel starvation. The impact of slight current disturbances on membrane degradation is hard to assess beforehand.

5

PEMFC and current ripple

This chapter describes where fuel cell current ripple originates, and its influence on the behavior of a fuel cell. Additionally, the literature with regard to the degradation of fuel cells with regard to current ripple is discussed.

In the pursuit of a longer lifetime for PEMFC everything that can have an influence on the processes inside a fuel cell is investigated. The current ripple that is introduced by the power electronics is one of the topics that has had some academic attention.

5.1. Source of current ripple in fuel cell systems

During the power conversion in the power electronics (see Section 3.4), disturbances are introduced into the electric signal, current ripple. The current ripple also travels through the fuel cell possibly influencing the electrochemical processes and fuel cell components.

In research investigating a distinction is often made between two types of current ripple, high frequency current ripple (>10 kHz) and low frequency current ripple (100 Hz - 120 Hz). [30]

5.1.1. High frequency current ripple

High frequency current ripple originates from the DC-DC conversion that happens in all fuel cell power electronics systems. The frequency of >10 kHz is related to the switching frequency (PWM) that is used in these converters. The simplest DC-DC converter that can be used with a fuel cell is the step-up boost converter. A diagram can be found in Figure 5.1. The fuel cell is represented by the voltage source on the left, the rest of the circuit consists of an inductor, a switch, a diode, a capacitor and finally the load on the right.

The current ripple trough the inductor (and the fuel cell) is determined by (5.1), where D is the duty cycle of the switch. It can be seen that current ripple through the FC is inevitable, only the inductance can be tweaked to change the magnitude of the current ripple. In Figure 5.2 the waveform of the current ripple through the inductor can be seen, the current raises when the switch is closed and decreases when it is opened.

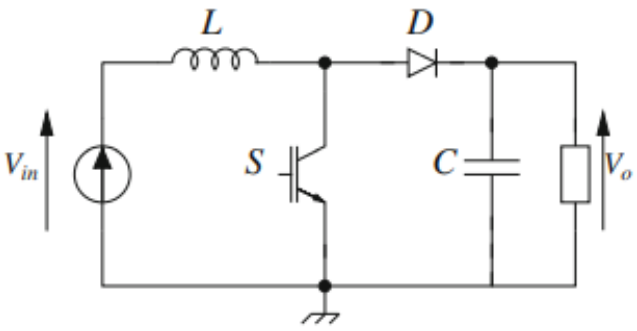

Figure 5.1: Diagram of a boost converter [15]

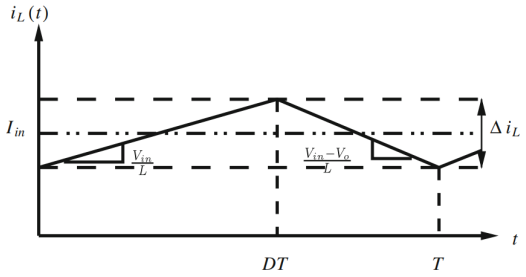

Figure 5.2: Boost converter current ripple [15]

$$\Delta i_L = \frac{D(1-D)V_o}{L_f} \tag{5.1}$$

There are many more types of DC-DC power converters (with more complex topologies) but there will always be current ripple. There are however methods to minimize the high frequency current ripple. Firstly, a passive approach can be used. A low pass RLC-filter can be applied between the fuel cell stack and the power converter to smooth out the disturbances. The downsides are that high power filters can become bulky and expensive, additionally it will introduce extra losses that decrease the efficiency of the overall power system. The second option is an active ripple reduction method. An example of this is a multi-phase DC-DC converter. While DC power in itself does not have a phase, the current ripple does. In Figure 5.3 it can be seen how multiple ripple phases evenly spaced out can decrease the current ripple to 1/N, where N is the number of phases [31]. The amount of phases that are feasible to implement is limited, more phases means more complexity and more switching losses.

5.1.2. Low frequency current ripple

Low frequency current ripple are harmonics originating from a single phase inverter. This can be explained using the energy balance between the input (fuel cell, DC) and the output (AC) of the inverter, see (5.4)). Equation 5.5 shows that the current drawn from the fuel cell is not constant but has a ripple with twice the frequency of the AC.

$$v_{\text{ac}}(t) = V_{\text{peak}} * \sin(\omega t) \tag{5.2}$$

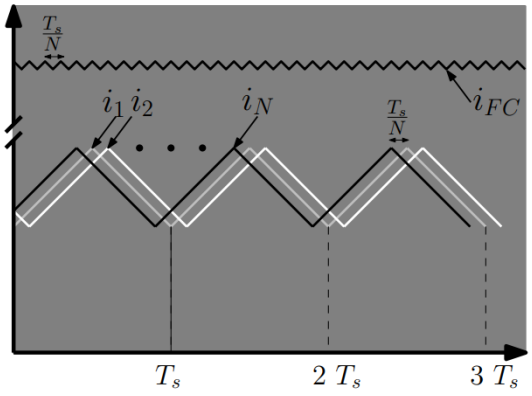

Figure 5.3: Interleaved boost converter current ripple [30]

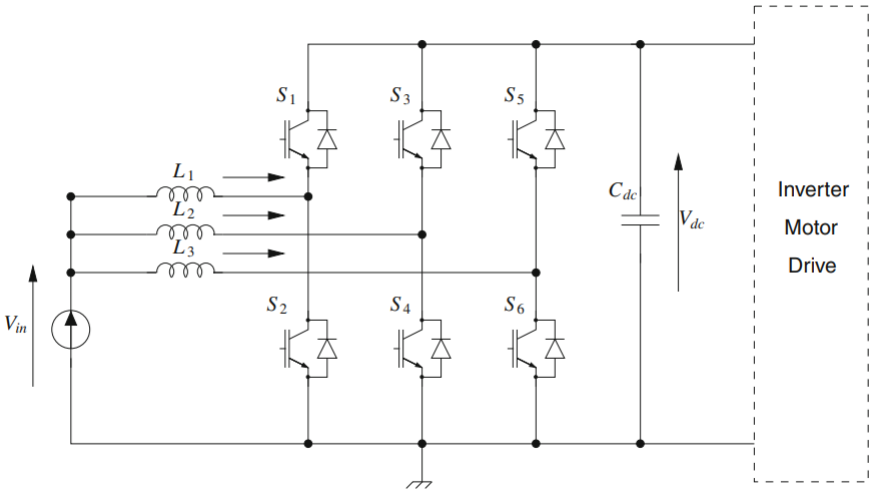

Figure 5.4: 3 phase bidirectional boost converter [15]

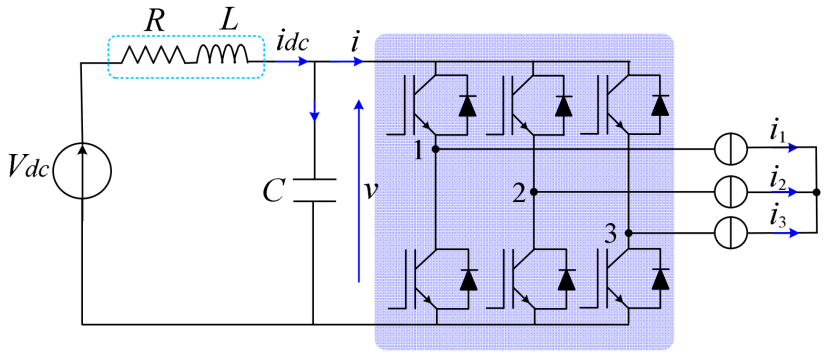

Figure 5.5: Three-Phae PWM inverter schematic [33]

$$i_{\text{ac}}(t) = I_{\text{peak}} * \sin(\omega t - \phi) \tag{5.3}$$

$$V_{\text{fc}} i_{\text{fc}}^{*} = v_{\text{ac}}(t) i_{\text{ac}}(t) = V_{peak} * \sin(\omega t) * I_{\text{peak}} * \sin(\omega t - \phi) \tag{5.4}$$

$$i_{\text{fc}}^{*} = \frac{V_{\text{peak}} I_{\text{peak}}}{2V_{\text{fc}}} \cos(\phi) - \frac{V_{\text{peak}} I_{\text{peak}}}{2V_{\text{fc}}} \cos(2\omega t - \phi) \tag{5.5}$$

An inverter will usually produce AC with a frequency of 50 or 60 Hz (typical electrical grid frequencies), the current ripple will then have a frequency of 100 or 120 Hz.

Low frequency can be reduced using similar approaches as high frequency ripple. A passive filtering method could work, but the size and power dissipation make this approach less than ideal, and the attention is shifting toward active methods [32]. They can be divided into two groups, the power conditioner self-controlling method and the current ripple injection method [32]. The self-controlling approach works by adapting (the control of) conventional power electronics to reduce current ripple. The second approach is injecting ripple into the system to cancel out the original current ripple. The current ripple injection is powered by a separate power source for example: capacitors, super capacitors or batteries. [30].

The ideal solution to this type of low frequency power ripple is using three phase AC instead of single phase AC. The extra phases give a constant power over time, negating the inherent current ripple shown in (5.5).

5.1.3. Three-phase PWM inverter

Three-phase PWM inverters are used in many applications, for instance in uninterruptible power supply systems or in grid-connected or independent energy generation systems. This means that fuel cells are very likely to be used together with three-phase inverters.

In Figure 5.5, the circuit for a three-phase PWM inverter can be seen, it consists of six pairs of switches and diodes. In this figure it is accompanied with a resistor, inductor and capacitor that represent the power source.

The maximum voltage ripple (peak-to-peak) on the DC-bus of a three-phase PWM inverter can be approximated using (5.6). The frequencies that make up the current

ripple are the switching frequency (f_s), its even multiples ($2*f_s$, $4*f_s$ etc.) and the side-bands around the odd multiples of the switching frequency ($f_s \pm 3$, $3*f_s \pm 3$, $5*f_s \pm 3$)[34].

$$\Delta V_{\max} \approx \frac{1}{8}\frac{I_o T_s}{C} \tag{5.6}$$

Where I_o is the amplitude of the current output of the inverter, T_s is the switching period and C is the capacitance of the power source.

These parameters depend strongly on the specific application of the fuel cells. The hypothetical implementation is a three-phase grid-connected fuel cell power generation system with a capacity of 500kW.

500 kW at 230V AC gives a current amplitude of 1025A, a switching frequency of 20kHz is assumed, giving a $T_s = 50\mu s$. Assuming a stack size of 96 fuel cells, and 6 parallel strings of 10 stacks (of 96 cells), the total capacitance of the fuel cell stacks is 62.5 mF (the capacitance of the fuel cells was determined to be 10F in Section 9.1.1). This leads to a current ripple of 0.1V peak-to-peak.

5.2. Influence of current ripple on PEMFC

When investigating the influence of current ripple on a fuel cell, you want to know what is going on inside the cell. Ideally without disassembling or breaking it. One could use the polarization curve of the cell(s), but it can be difficult to extract the influences of the different fuel cell components on the performance from there. Another consideration is that the polarization curve itself represents the operation of the fuel cell in relatively static circumstances, which can lead to mistakes when trying draw conclusions that relate to other conditions (current ripple for example [35]).

5.2.1. Electrochemical impedance spectroscopy

A more intricate research tool is electrochemical impedance spectroscopy (EIS), which is therefore an important tool in experimental research of fuel cells. The basic concept is that a DC load with a sinusoidal perturbation is applied to the fuel cell, its response is then analyzed. EIS can be performed in potentiostatic or galvanostatic mode. In potentiostatic mode, an AC potential pertubation is applied to the FC while the current response is measured. However, there is a risk of overloading the FC or the measuring equipment because a small change in potential can lead to a large current change. In galvanostatic mode, an AC current pertubation is applied to the FC while the potential response is measured. This method allows more precise control of the currents in the FC, leading to much less risk of overloading the equipment. The EIS measurements can be used for multiple purposes [36]:

1. provide microscopic insight into the fuel cell, which is useful for optimizing fuel cell structures and operating conditions.

2. facilitate modeling the fuel cell as an equivalent circuit which can then be used to obtain the electrochemical parameters of the fuel cell.

3. investigate the performance of the individual components of the fuel cell (membrane, anode, cathode, etc.) which can be used to identify the degradation of components.

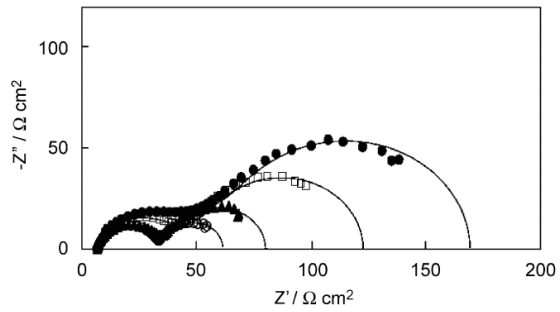

Figure 5.6: Example of Nyquist plots of a electrochemical impedance spectrometry experiment [36]

4. investigate different electrode processes, such as interfacial charge transfer or mass transport.

EIS is typically performed between the frequencies of 1 mHz and 100 kHz. The phenomena that can be studied are, in order of decreasing frequency (and the associated FC component(s)): ohmic resistances (membrane, electrodes), electrochemical charge transfer (catalyst), mass transfer (active layer, GDL) [36, 37].

The results of EIS are usually presented in a Nyquist plot such as Figure 5.6 or as the parameters of an equivalent circuit.

5.2.2. Double layer capacitance

The particular shape of the curves in Figure 5.6, is in part due to the double layer capacitance that occurs at both electrodes in a fuel cell. When two different materials touch, there be a transfer of charge and a build-up of charge on the surfaces. This also happens in fuel cells at the electrodes because of diffusion, the reactions at the electrodes (that include the charged particles) and the applied voltages.[1] At the cathode, (see Figure 5.7) electrons will gather at the surface of the electrode and protons are attracted to the surface of the electrolyte. There they can take part in the cathode reaction (together with oxygen). More electrons and protons at the surface means that the reaction can occur more easily. However, the build up of charged particles generates and electrical voltage, this is the activation voltage drop that is mentioned in Section 2.7. The presence of the double charge layer has affects the dynamic properties of the fuel cell, it acts as a capacitor. Because of the very short distance between the differently charged particles, the capacitance can be as high as multiple Farads [1].

5.2.3. Influence of ripple on performance

Gemmen [38] was one of the first to investigate the influence of current ripple on proton exchange membrane fuel cells. His approach was purely theoretical, using simulations. The bulk reactant conditions were modeled as well as the mass transport occurring within the electrodes. It was found that the bulk reactant conditions are not significantly impacted by typical inverter loads. However, oxygen transport to the cathode was affected by current ripple with a frequency of 120 Hz and lower. To minimize the performance loss, a maximum current ripple factor of 4% was advised. Ripple with a frequency higher than 120 Hz were also deemed to have no influence

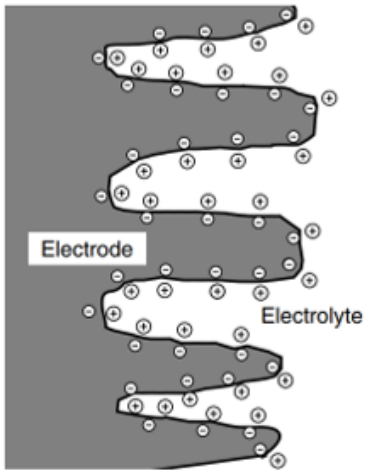

Figure 5.7: Schematic depiction of the charge double layer at a PEMFC cathode.[1]

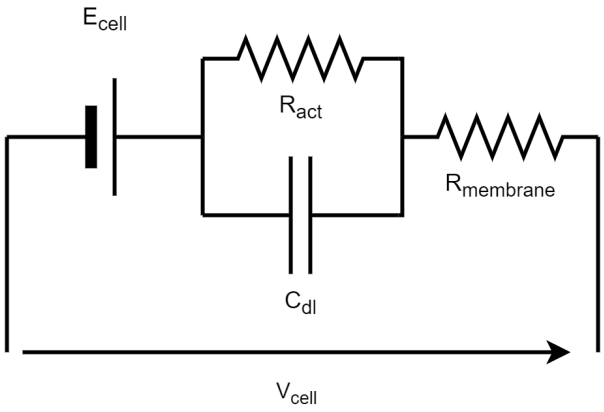

Figure 5.8: Simple equivalent electrical circuit for FC with equivalent capacitor

on FC behavior.

Another approach is through modeling the fuel cell as an equivalent electrical circuit based on EIS measurements. Two simple FC models can be seen in Figure 5.8 and 5.9. The resistor-capacitor couple is an important part of every FC equivalent circuit, it represents the activation phenomena at the electrodes. Figure 5.9 uses a resistor-capacitor pair for both electrodes, while Figure 5.8 uses an equivalent resistor capacitor pair. The other resistor represents the ohmic resistance of the membrane and the electrodes.

Choi [39] did this for two different fuel cell stacks. At a ripple frequency of 120 Hz, the reduction in available power of the fuel cell was calculated and experimentally tested. The power loss due to current ripple can be calculated with the equivalent circuit, (5.7) uses the real part of the impedance of the circuit and the rms of the ripple current. The power loss due to current ripple was up to 9% for 100% ripple but was reduced to 1% when the ripple is limited to 30%.

Zhan et al. [40] also did experiments regarding the influence of current ripple on stack efficiency. They found that a ripple of 10% gives a higher efficiency when compared to a ripple of 25%. It was also found that a higher ripple frequency results in

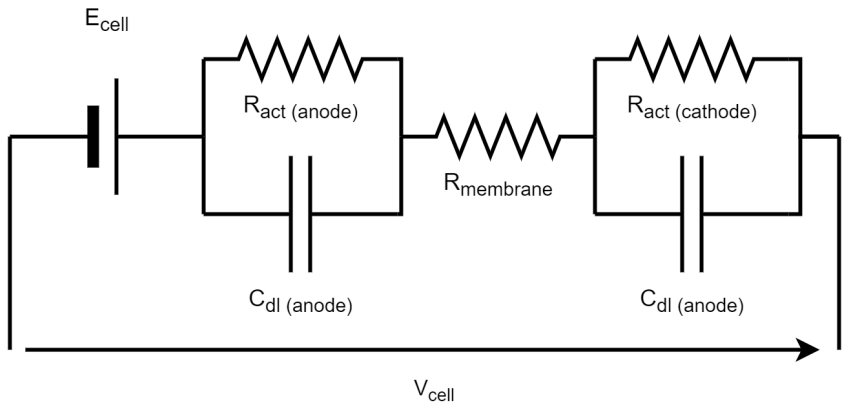

Figure 5.9: Simple equivalent electrical circuit for FC

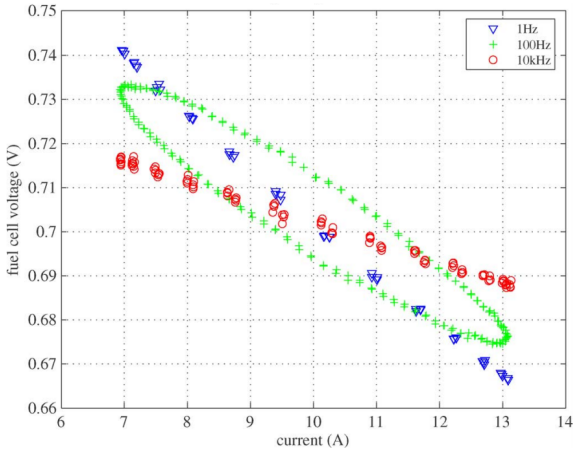

Figure 5.10: FC potential response to current ripple [7]

lower efficiency losses (in the range of 50Hz - 400Hz). The loss of power resulted in higher stack temperatures, which could accelerate degradation.

$$P_{\text{ripple}} = \text{Real}(Z(j\omega))I^2_{\text{ripple}} \tag{5.7}$$

Fontes et al. [7] show what the potential response of a fuel cell is when a large current ripple (60%) is applied. In Figure 5.10 three distinct possibilities are shown. When the ripple frequency is much higher or lower than 100 Hz the voltage response simply follows a straight line. At 100 Hz, a hysteresis effect occurs, which is related to the dipole from the double layer capacitance and the activation resistance. The time constant of the dipole depends strongly on the current density.

Fontes et al. [7] also performed simulations and experiments with a buck chopper directly connected to the fuel cell with a current ripple of up to 100% at 19.7kHz. They found that the double layer capacitor functioned as a filter for high frequency disturbances, the resulting voltage ripple was 6%.

It was mentioned before that the performance loss due to current ripple can be calculated using the equivalent circuit of the fuel cell, using EIS to determine the parameters. But Electrochemical impedance spectroscopy is a difficult technique, it requires advanced instrumentation, stable fuel cell conditions, and a lot of time (sometimes

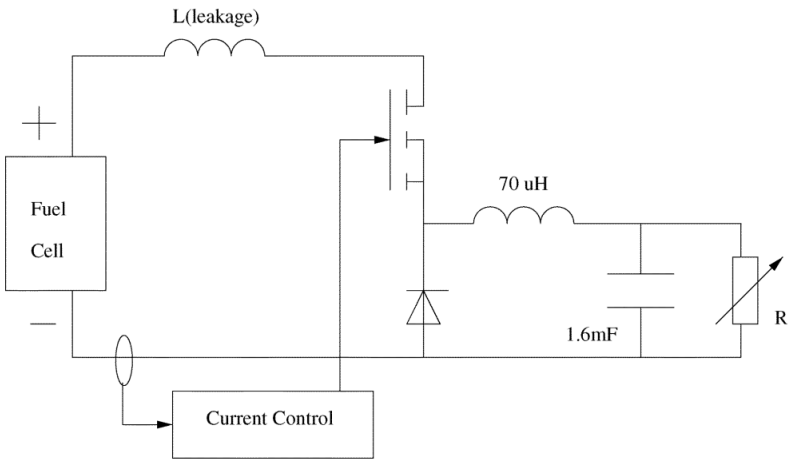

Figure 5.11: Schematic of buck chopper attached to fuel cell [7].

many hours). Ferrero, Marracci, and Tellini [35] compared this procedure with equivalent circuit parameters obtained by analyzing the polarization curve of the FC, which is much easier to obtain. They found that you can use the polarization curve to approximate ripple losses, but the hysteresis behavior depends on the exact ripple form. IES should be used for a more accurate estimation of ripple losses.

Other than just the performance impact of current ripple, or the relation between current ripple and voltage ripple, the influence of current ripple on the processes inside a fuel cell is also interesting. Xu et al. [14] built a multi-scale model to study the impact of high frequency (20kHz) current ripple on the internal states of a fuel cell. It was found that only the processes that are directly related to the fuel cell current are influenced. This includes important variables such as the FC voltage, cathode polarization, ohmic losses and the stoichiometry of hydrogen and air. Variables that are related to the mass transfer processes are only affected slightly, examples are the partial pressures of the gasses, membrane hydration levels and liquid water saturation ratio.

5.2.4. Ripple and degradation

The influence of current ripple on FC performance can be determined experimentally or using an equivalent circuit model (as Choi [39] did for example). Unfortunately, investigating the degradation of fuel cells due to current ripple is more complex. As mentioned before, because of the tightly coupled processes and components inside a fuel cell, finding the precise degradation mechanisms is difficult. Additionally, degradation experiments take a long time because the fuel cells need to be running for thousands of hours.

Despite these obstacles, experimental research has been done with regard to fuel cell degradation for both low frequency and high frequency current ripple. Zhan et al. [40] did a basic experiment comparing the lifetime of a fuel cell stack that was exposed to low frequency current ripple to a reference stack. The stack exposed to current ripple failed after ~2500h while the reference stack ran for more than twice as long (~5500h). No additional failure analysis or EIS experiments were performed.

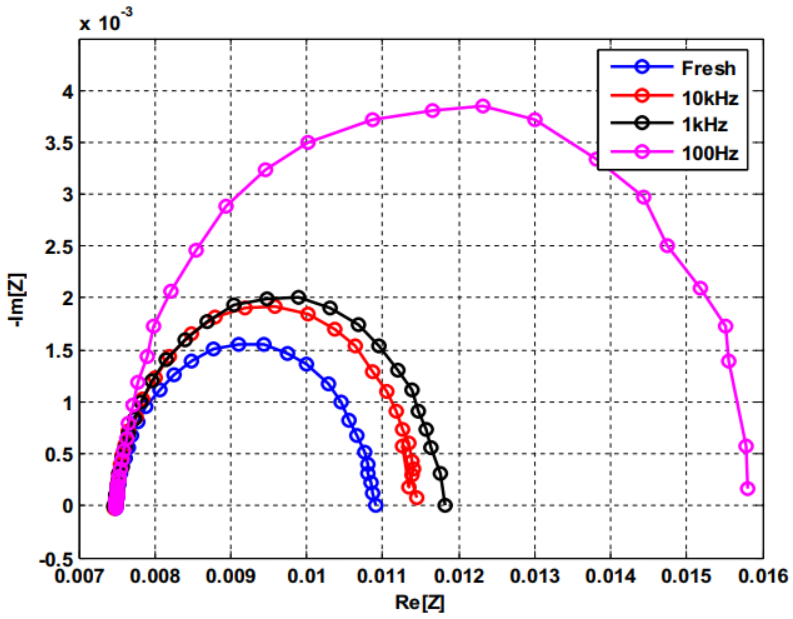

Figure 5.12: IES comparison for FC subjected to current ripple with different frequencies for 100h [41]

A more thorough investigation into degradation associated with both high and low frequency current ripple was performed by Kim et al. [41]. Three different ripples were compared, with a frequency of 100Hz, 1 kHz and 10kHz, and an amplitude of 20A (100%). The experiments ran for a duration of 100h, which is a short period of time. The cells were compared using EIS, in Figure 5.12 it can be seen that the fuel cell that was subjected to 100 Hz ripple, performs significantly worse than the other fuel cells. Kim et al. [41] pointed towards membrane dehydration and electrode flooding as possible degradation mechanisms for low frequency current ripple.

Wahdame et al. [42] reported some interesting behavior of a PEMFC stack that was subjected to a high frequency current ripple (1000 Hz, amplitude of 50A (+/- 10%)). For the first 100h of testing the stack performed better than the reference stack. After that phase, the performance degradation starts. After 1000h the performance of the reference stack had decayed with 280 µV/h. The stack that was subjected to current ripple decayed with 308 µV/h, an increase of 10%. An EIS analysis showed that the internal FC resistance (measured at very high frequencies) only changes slightly, from 1.4 mΩto 1.6 mΩ.

A similar experiment was performed by Gerard et al. [37], a stack of 5 cells was subjected to a current ripple of 40% at 5 kHz for a duration of 590h (until a membrane failure occurred). The reference stack did survive until 1000h. Apart from the lifetime, increased reversible degradation was observed.

In Figure 5.13 it can be seen that the voltage decay resets when the cells are characterized. The OCV degradation is similar for the ripple stack and the reference stack. The cells were compared before and after the characterization process using EIS. It was found that the reversible degradation was caused by reduced water management in the GDL and the active layer. Before the experiment and after the failure the membrane performance and platinum activities were investigated using voltammetry (measuring the FC current while the potential is varied). Unfortunately, the fuel

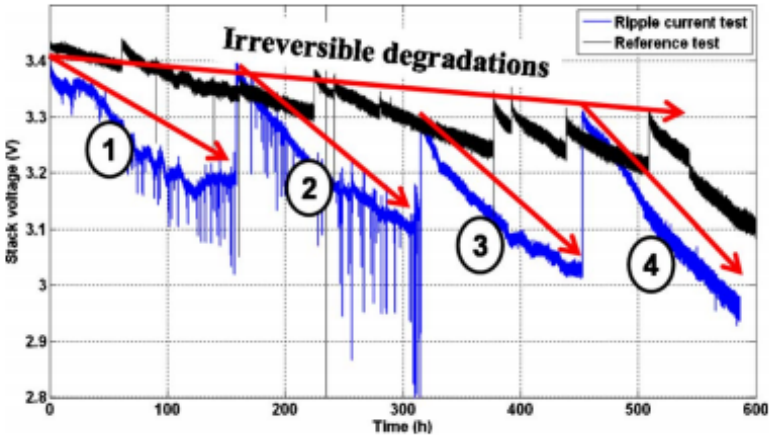

Figure 5.13: Stack potential during current ripple test [37]

Author	Frequency	Base current	Amplitude	Relative ripple
Gerard et al. [37]	5kHz	110A	22A	40%
Kim et al. [12]	100Hz, 1kHz, 10kHz	20A	10A	100%
Wahdame et al. [42]	1kHz	250A	25A	20%
Uno and Tanaka [43]	1Hz - 1kHz	0.75V	0.15V	40%

Table 5.1: Parameters of current ripple degradation experiments. Base current is the current associated with the DC load. Base Relative ripple is defined as the ratio between the ripple and the base current: $\frac{\Delta I_{\text{ripple-peak-to-peak}}}{I_{\text{base}}} * 100\%$. Uno and Tanaka [43] performed their experiments using the FC voltage instead of current, due to the non-linear behaviour of FC's, the parameters cannot be easily converted.

cells were damaged in such a way that the platinum activity could not be calculated. It was clear however, that all five of the membranes were severely damaged. They showed increased current permeation, increased resistance or both. Additionally, a model-based investigation was done into the influence of current ripple on local conditions in the fuel cell, the membrane temperature was highlighted, but no conclusions could be drawn from the results.

Specific experimental research could probably give the most insight into the degradation of fuel cell components due to current ripple, but it is currently lacking.

One example is the work of Uno and Tanaka [43], they investigated the impact of current ripple on catalyst degradation. They noted that current ripple leads to potential cycling, which is known to be a factor in catalyst degradation. While the voltage delta for realistic current ripple is probably smaller than that of start/stop cycling or operational transients, it could have a similar impact on the ECSA. The experiments were performed on single cells, the current ripple being 0.30V around an average of 0.75V, with frequencies between 1Hz and 1kHz. They found that for frequencies lower than 100Hz, the current ripple induced potential cycles resulted in ECSA losses that are comparable to those of conventional potential cycling, that emulates load variation or start/stop cycles. Above 100 Hz, the ECSA losses were similar to the reference case with a purely DC load. Carbon corrosion was investigated and not considered to be factor that influences the frequency dependent ECSA loss.

5.3. Conclusion

Power electronics can introduce two types of current ripple into a fuel cell, their differences being the frequency and the source. High frequency current ripple is associated with the switches used in power converters, both in DC-DC, and DC-AC conversion. The frequency of this current ripple is the same as the PWM frequency of the switches, which is usually 10 kHz or higher. Low frequency current ripple is specifically caused by DC-AC conversion by a single phase inverter. The associated frequency is twice the AC frequency, i.e. 100 Hz for the European grid. For both ripple types the current ripple can be reduced using filtering or active methods (adding phases) but this comes at the cost of added volume, weight, complexity and reduced efficiency.

An important factor in the response of a fuel cell to current ripple is the double layer capacitance. This effect that occurs at the electrodes lessens the effect of high frequency current ripple on fuel cells by functioning as a low pass filter. Low frequency current ripple, on the other hand, can have a significant impact on fuel cell performance (maximum power and efficiency), mainly at high ripple amplitudes.

The literature is less clear with regard to the relation between current ripple and fuel cell degradation. Multiple experiments have been performed to investigate this, with different ripple frequencies, ripple amplitudes and relative ripple sizes. The results for high frequency current ripple ranged from slightly accelerated performance degradation to significantly increased reversible degradation and early membrane failure. Low frequency voltage ripple (related to current ripple but not directly comparable) could result in significant loss of ECSA according to one experiment [43].

6

Conclusion

Proton exchange membrane fuel cell may play a big role in transition away from fossil fuels. They convert hydrogen and air into electric energy and water, without any harmful emissions. While that can be said about more fuel cell concepts, PEMFC has some characteristics that make it easier to implement. The low power-to-volume and power-to-weight ratios and the cold start capability can be very important for certain applications, vehicles for example.

In Section 2, the basic components of a PEMFC were shown, the electrodes with the catalyst particles and the membrane. How these components turn hydrogen and oxygen into electricity was also explained.

While the principles of a PEMFC are simple, to keep it running smoothly is more complex. A lot of auxiliary equipment and control systems are necessary to supply the reactants at the correct amounts and hydration level and to keep the internal fuel cell conditions optimal.

An important barrier that is left for widespread adoption of proton exchange membrane fuel cells is the durability. Due to the reactive environment inside the fuel cell (temperature, the presence of catalysts, hydrogen and oxygen), the components of fuel cells degrade when they are used, especially in situations with dynamic loads or start-stop cycling.

A specific cause for increased degradation is current ripple. Fuel cells are always used in conjunction with power electronics to boost and stabilize the voltages. The power electronics will introduce disturbances into the current that the FC needs to deliver. These disturbances can influence the behavior of the FC or even accelerated the degradation. In Section 5.1 it was explained that there are two types of current ripple that can be distinguished between in this context. Low frequency current ripple is caused by the conversion of DC to AC by an inverter, it has twice the frequency of the AC signal, so often 100 Hz or 120 Hz. High frequency current ripple is caused by high frequency switching (>10 kHz) in the power electronics, for example in DC-DC converters. Both types of current ripple can be counteracted using passive filters or active ripple reducing methods. But these methods can decrease overall efficiency, take up valuable space, increase the complexity of the electric topology and control algorithms and in general add costs to the system.

A balance should be found between the decreased efficiency, increased complexity and increased costs that come from counteracting the current ripple on one

hand, and the decreased performance and accelerated degradation on the other hand. Therefore it is important to know the precise influence of current ripple on fuel cell performance and degradation.

Both simulations and experiments have shown that low frequency current ripple can have an effect on the power that a fuel cell is able to deliver (and the efficiency of a FC), the impact can be up to 9% performance loss at high ripple amplitudes. High frequency current ripple has no significant influence on the performance of a fuel cell. Aside from the performance, HFCR only affects FC processes that are directly linked to the current, the FC voltage and the flow of protons and water through the membrane.

The degradation of fuel cells due to current ripple has mainly been investigated using experiments. For low frequency current ripple, the literature points towards to reduced lifetime [40], accelerated degradation in general [41] and specifically accelerated catalyst degradation [43]. For high frequency current ripple, the influence on the durability of a fuel cell is less clear. The findings range from no significant impact [41, 43], or a 10% faster degradation [42], to early critical membrane failure and significantly increased reversible degradation [37]. Additionally, because of the limited number of experiments that has been performed, little can be said about the influence of the ripple amplitude and frequency (within the domain of HFCR) on the degradation.

6.1. Research Gap

Based on the analyzed the research gap can be concluded. The first research gap is the absence of a quantitative analysis on the effect of current ripple on proton exchange membrane fuel cell degradation. The research that has been performed is very specific, with a single ripple frequency, current density and ripple amplitude. Especially the relation between current ripple degradation and the ripple amplitude would be very valuable in the design process of power electronics for fuel cell systems. It would help towards a better understanding of the significance of current ripple degradation when compared to other degradation accelerating conditions (load transients or start-stop cycling).

The second research gap is the absence of an identified or proposed degradation mechanism associated with high frequency current ripple. Research has been done into the overall degradation of fuel cells through high frequency current ripple, but aside from pointing membrane degradation in general [37], no degradation mechanisms have been proposed to cause the decay associated with high frequency current ripple. Identification of the main high frequency ripple degradation mechanisms could help to find ways to strengthen fuel cells against the degradation, and also help fill in the first research gap.

6.2. Research Objective

With the research gaps in mind, it is possible to establish a suitable direction for novel research. The research aims to increase the knowledge of the influence that current ripple has on the internal components and processes of a proton exchange membrane fuel cell.

When considering the subject for new research into the impact of current ripple

on fuel cells, it should be noted that while low frequency current ripple arguably has the largest influence on fuel cell degradation, focusing on just the low frequency current ripple has a limited relevance for a lot of applications. It requires a single phase AC-inverter to be present in the system, but conversion to three phase AC is more suitable for a lot of fuel cell implementations. Therefore this research will not be the limited to a specific current ripple frequency, but take the whole range of possible ripple frequencies into account.

A model will be built to approximate the degradation of a PEMFC due to current ripple. This model will take the degradation of one fuel cell component into account, the catalyst. As mentioned before, catalyst degradation is the most likely option for ripple induced decay. It is known that potential fluctuations accelerate catalyst degradation, and current ripple causes exactly that. Meanwhile the degradation mechanisms associated with the carbon electrode and the membrane are much harder to link to current ripple.

This leads to the following research objective:

Develop a model of the current ripple induced catalyst degradation in a proton exchange membrane fuel cell.

This objective is accompanied by two sub-questions:

- *What is the impact of ripple degradation compared to steady state FC degradation?*
- *How does the ripple frequency influence ripple degradation?*

The model will be build up out of two parts. The first sub-model concerns the catalyst degradation that occurs when a fuel cell is subjected to a stable DC load. Fuel cells continually degrade when under load, and it is interesting to compare the contribution of the stable load and the current ripple to the total catalyst degradation because they are both degradation sources that are 'active' during most of the lifetime of the fuel cell.

The second module models the catalyst degradation due to current ripple. This sub-model will be based on fuel cell degradation experiments performed in a lab. It will take into account the working time, ripple frequency and ripple amplitude, and predict the ECSA degradation.

II

Modeling

7

Modeling methodology

In this chapter the modeling methodology is described. Modeling fuel cells is a complex subject and a many different approaches have been described in literature. This chapter outlines some of the challenges of fuel cell modeling and gives the structure of the created model.

7.1. Fuel cell modeling

A model of a fuel cell (stack) is very useful when implementing fuel cells in the real world, for designing the equipment that interacts with the fuel cells (BOP), for developing controllers for fuel cells, and for research into the inner workings of fuel cells. These applications can use different kinds of models, which like all model reside on the spectrum between black box models and white box models. Black box models generally use empirical data to mimic the behaviour of a fuel cell anything from simple regressions to neural networks. A benefit of these kind of models is that they are usually very quick (computationally light) which is important when a model is implemented in a controller. White box models are build up using the governing equations of the system. It should ideally be an exact mathematical copy of the original system, which gives a lot of insight in the inner workings. The problem is that fuel cells are very complex systems, which are very difficult to fully capture using a set of equations.

There are a multitude of processes occurring concurrently inside a fuel cell. An overview can be found in Table 7.1.

Not only are some processes in itself not fully understood, they are coupled, introducing more complexity to the system. An additional problem is the difference of the timescales and length scales in which the processes take place. Figure 7.1 gives an

Location	Processes
membrane	proton transport, water transport, gas permeation
catalyst layer	electrochemical reactions, transport in porous media, transport in agglomerates
GDL	two-phase flow, multi-component transport in porous media

Table 7.1: Processes inside a PEMFC [20]

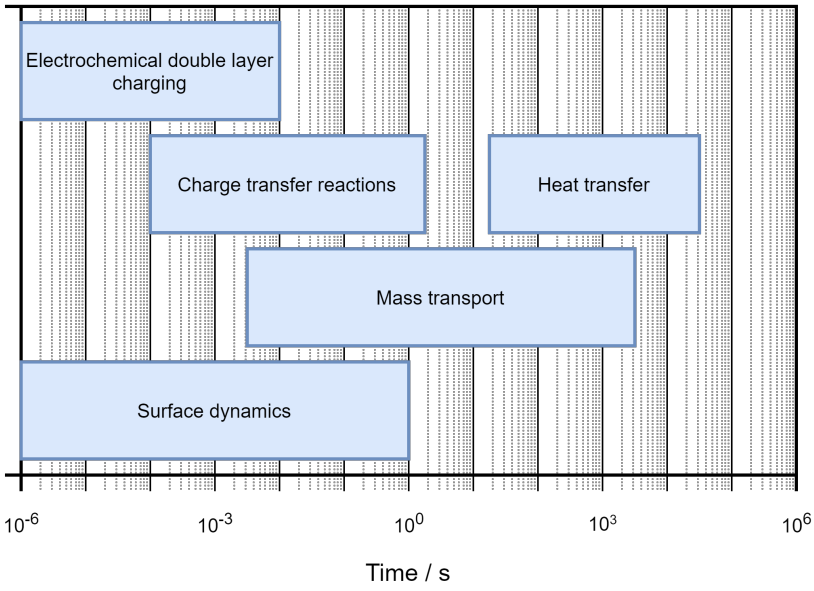

Figure 7.1: Timescales of processes in fuel cells [20]

overview of the timescales of a number of different processes inside a fuel cell. To accurately simulate a (part of a) fuel cell, all relevant processes (on their respective timescales) need to be modeled and coupled appropriately. Many different PEMFC models have been developed of the different fuel cell components, specific processes or degradation mechanisms, or full system level models. Jahnke et al. [20] gives a comprehensive overview of modeling of PEMFC

7.1.1. Fuel cell current ripple modeling

In theory, most fuel cell models could be used with current ripple. Since almost all models include the current drawn from the fuel cell, one could apply a current ripple to it. Unfortunately, fuel cell models usually are built for a specific purpose, and changing the conditions drastically (by applying a current ripple) will not give in useful results. One important factor in this problem is the double layer capacitance, which influences the dynamic behavior.

One type of model is already used to study FC responses to current ripple, Equivalent electrical circuits. EEC's can be used when designing electrical equipment that interfaces with a fuel cell. In that case it is necessary to know how the fuel cell behaves electrically. This includes characteristics as the internal resistance, or more importantly, the impedance.

The most elegant way to approach this is to model the fuel cell using electrical components. For fuel cells, different EECs can be used with different complexity levels. Two examples were mentioned before, Figure 5.8 and Figure 5.9. A more complicated EEC can be seen in Figure 7.2.

The values for the components of the equivalent circuit need to be found using experiments, this can be done using EIS. The parameters (resistances, capacitances and inductances) of the EEC are then fitted to the results of the EIS. There is a limit to the information that can be extracted from an EIS experiment, this is why in practice the EEC shown in Figure 5.8 is often used.

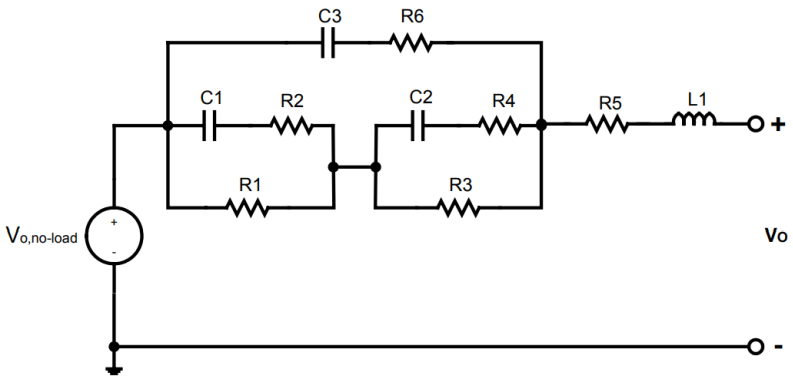

Figure 7.2: EEC of fuel cell [39]

One drawback of these EECs is that they are specific to the state and configuration of the fuel cell, the temperature, gas composition, membrane hydration level and pressure, to name a few. Most importantly, an EEC is specific to the fuel cell current at which it is fitted. They do not incorporate the polarization behavior of a fuel cell. Additionally, they give little information about what is happening inside the fuel cell.

7.2. Fuel cell degradation modeling

The degradation of fuel cell components does not appear in regular fuel cell models. The degradation mechanisms must be explicitly modeled. Many different fuel cell degradation models have been built for the different degradation mechanisms of all the fuel cell components (see Jahnke et al. [20] for an overview). No models regarding current ripple damage to fuel cells have been built yet. Which is not surprising, due to the lack of knowledge of the degradation mechanisms associated with current ripple.

7.3. Model structure

The goal of the model is to predict the ECSA degradation rate of a fuel cell when it is subjected to a certain current ripple. The model will take the parameters that describe a current ripple: the amplitude, the average current and the frequency, and will calculate the degradation rate. This will be called the ripple shape in this report, not to be confused with whether the ripple is sinusoidal, triangular, square etc., which is not taken into consideration in this model. The model consists of two modules, one for calculating the ECSA degradation associated with a constant load (the average current), and one that calculates the ECSA degradation due to the ripple. A schematic overview can be seen in Figure 7.3.

The steady state module was introduced by Ao et al. [44], it is based on the transformation of individual catalyst particles due to electrochemical dissolution, chemical dissolution and Ostwald ripening. The current ripple degradation module is based on based on ECSA degradation data from an experiment, which is extrapolated to different ripple shapes using a fuel cell impedance model.

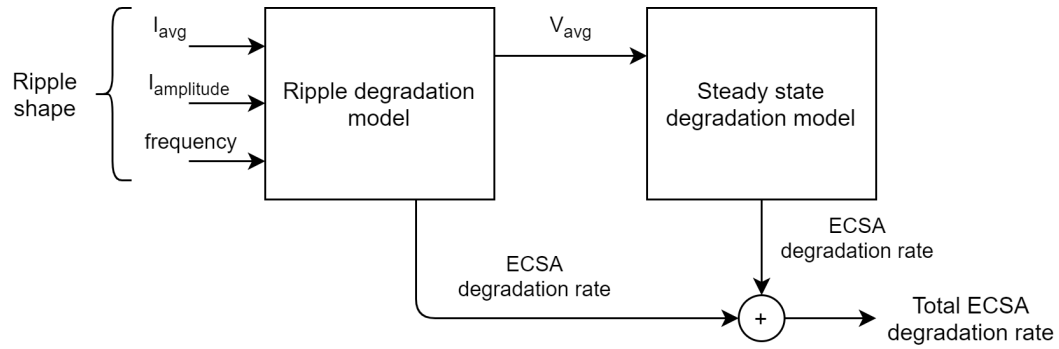

Figure 7.3: Schematic overview of model structure

The construction of this model requires a number of assumptions:

- No spatial differences within the electrodes.
- Input and output cell pressures are constant and equal.
- Gas diffusion is in steady state.
- Temperature and hydration are constant and known.
- Ripple ECSA degradation scales with voltage amplitude of the ripple.
- Ripple frequency does not directly influence ECSA degradation rates (only through its effect on the voltage amplitude).

7.4. Conclusion

In this chapter the complexity of fuel cell modeling was outlined. Modeling of fuel cells is an important factor fuel cell research because of the difficulties of investigating the processes that are going on inside fuel cells. But the many different processes (with wildly different timescales), which can by themselves already be difficult to model, influence each other in a multitude of ways. This leads to the need for multiple coupled modeling methods to create a comprehensive fuel cell model. Modeling the degradation of fuel cells is a separate subject, with specific models for all degradation mechanism.

A model type that is relevant for fuel cell modeling related to current ripple, is an equivalent electrical circuit. They explicitly model the dual layer capacitance, which is important for the accuracy of the dynamic response.

Currently, no models exist on the subject of fuel cell degradation due to current ripple.

The model that is introduced in this report predicts the ECSA degradation rate based on the current ripple the fuel cell is subjected to. The model is built up using two modules, the steady state degradation module and the current ripple degradation module. The steady state module calculates the degradation based on the average load. The current ripple degradation module uses experimental data and a fuel cell impedance model to predict the ECSA degradation due to the ripple.

8

Steady state degradation model

This chapter discusses the process of modeling the catalyst degradation of a fuel cell under steady state conditions. The ECSA of the fuel cell will be modeled over time when exposed to a predetermined current and potential. Firstly, the implemented model will be explained, followed by the estimation of the necessary parameters. Finally, the results of the steady state model are discussed.

8.1. Catalyst transformation model

The used steady state degradation model was developed by Ao et al. [44]. The base of the model are the platinum nano particles that function as the catalyst in a PEMFC. A number of particles are created, and pathways for platinum molecules to detach from (or attach to) the individual particles are modeled. The modeled mechanisms are: electrochemical dissolution, chemical dissolution and Ostwald ripening. Looking back at Section 4.1, it can be seen that the coalescence of Pt particles and the detaching of Pt particles from the carbon support due to carbon corrosion are not taken into account.

The dissolution and deposition of platinum on the particles changes their size, and consequently the ECSA. This is the most important output variable of the model. Other information that can be extracted from the model is the particle radius distribution (PRD), which is a parameter that gives some more insight in the state of the catalyst.

The general principle of the model can be seen in (8.1). Every catalyst particle i has a certain number of platinum molecules (n) and for every time step (j) it is calculated how much Pt molecules the different degradation mechanisms remove from (or add to) each catalyst particle. The particles initially consist of $n_{i,0}$ Pt molecules, which is determined by an initial particle radius distribution.

$$n_{i,j} = n_{i,j-1} + \Delta t \sum v(r_{i,j}) \tag{8.1}$$

In this equation Δt is the time step length and $v_{i,j}$ is the velocity of the reactions.

Four reactions are explicitly modeled, their reaction speeds are given by v_{1-4}. Electrochemical dissolution ((8.2), earlier introduced as (4.1)) with associated speed v_1, the pair of reactions responsible for chemical dissolution ((8.3) (v_2) and (8.4) (v_3))

and Ostwald ripening (v_4). The reaction speeds are a function of the radius of the associated particle.

$$\mathrm{Pt} \leftrightarrow \mathrm{Pt}^{2+} + 2e^- \tag{8.2}$$

$$\mathrm{Pt} + \mathrm{H_2O} \leftrightarrow \mathrm{PtO} + 2\mathrm{H}^+ + 2e^- \tag{8.3}$$

$$\mathrm{PtO} + 2\mathrm{H}^+ \leftrightarrow \mathrm{Pt}^{2+} + \mathrm{H_2O} \tag{8.4}$$

Reaction (8.3) creates a PtO layer at the surface of the particles, which influences Reactions 8.2 (by reducing the amount of Pt available for dissolution) and 8.4 (which dissolves the PtO). Therefore it needs to be incorporated into the model, the amount of PtO molecules on particle i at time step j is represented by $m_{i,j}$.

The Pt dissolution and Ostwald ripening reactions can be put into (8.5), which gives the transformation rules for Pt.

$$n_{i,j} = n_{i,j-1} + \Delta t(-v_1(r_{i,j}) - v_2(n_{i,j}) + v_4(r_{i,j}) \tag{8.5}$$

The amount of PtO molecules on a particle can be calculated using (8.6).

$$m_{i,j} = m_{i,j-1} + \Delta t(v_2(r_{i,j}) - v_3(r_{i,j})) \tag{8.6}$$

The reaction speeds (v_{1-4}) need to be calculated at every step for every particle because the reaction depends on the particle radius and PtO covering.

The velocity of (8.2) can be calculated using (8.7).

$$v_1(r_{i,j}) = (1 - \theta_{i,j-1})k_1(r_{i,j-1})\exp\left(\frac{F(E - E_1(r_{i,j-1}))}{2RT}\right) \tag{8.7}$$

Where

$$k_1(r_{i,j-1}) = k_1^{\infty}\exp\left(\frac{\beta\gamma V_{\mathrm{Pt}}}{RTr_{i,j-1}}\right) \tag{8.8}$$

$$E_1(r_{i,j-1}) = E_1^{\infty} - \frac{2\beta\gamma V_{\mathrm{Pt}}}{Fr_{i,j-1}} \tag{8.9}$$

With the following parameters:

θ Fraction of the particle covered in PtO [-].

k_1 Reaction rate constant of (8.2) [s^{-1}].

F Faraday constant of 96,485 C mol^{-1}.

E Electrical potential of the fuel cell [V].

E_1 Equilibrium potential of (8.2), which can be calculated using (8.9) [V].

R Ideal gas constant of 8.314 J $mol^{-1}K^{-1}$.

T Temperature of the fuel cell [K].

k_1^{∞} Equilibrium rate of (8.2) for bulk Pt (tuning parameter) [s^{-1}].

β Proportional constant between 0 and 1 [-].

γ Interfacial surface tension ($\beta\gamma = 1.2$ j m^{-2}) [45].

V_{Pt} Molar volume of Pt (9.09e-6 m^3mol^{-1} at 20°C).

E_1^{∞} Equilibrium potential for Pt bulk 1.188V [22].

The velocity of (8.3) can be calculated using (8.10).

$$v_2(r_{i,j}) = (1 - \theta_{i,j-1})k_2(r_{i,j-1})\exp\left(\frac{F(E - E_2(r_{i,j-1}))}{2RT}\right) \tag{8.10}$$

Where

$$k_2(r_{i,j-1}) = k_2^{\infty}\exp\left(\frac{\beta\gamma V_{\mathrm{Pt}}}{RTr_{i,j-1}}\right) \tag{8.11}$$

$$E_2(r_{i,j-1}) = E_2^{\infty} - \frac{2\beta\gamma V_{\mathrm{Pt}}}{Fr_{i,j-1}} \tag{8.12}$$

With the following parameters:

k_2 Reaction rate constant for (8.3) [s^{-1}].

E_2 Equilibrium potential of 8.3 [V].

k_2^{∞} Equilibrium rate constant of (8.3) (used as tuning parameter) [s^{-1}].

E_2^{∞} Equilibrium potential of (8.3) for Pt bulk (0.98V).

The velocity of (8.4) can be calculated using (8.13).

$$v_3(r_{i,j}) = \theta_{i,j-1}k_3(r_{i,j-1})\frac{c_{\mathrm{H+}}}{c_{\mathrm{H+}}^{\mathrm{ref}}} \tag{8.13}$$

Where

$$k_3(r_{i,j-1}) = k_3^{\infty}\exp\left(\frac{\beta\gamma V_{\mathrm{Pt}}}{RTr_{i,j-1}}\right) \tag{8.14}$$

With the following parameters:

k_3 Reaction rate constant for (8.4) [s^{-1}].

k_3^{∞} Equilibrium rate constant of (8.4) (used as tuning parameter) [s^{-1}].

$c_{\mathrm{H+}}$ Concentration of H^+ [mol L^{-1}].

$c_{\mathrm{H+}}^{\mathbf{ref}}$ Reference concentration of H^+ (1 Mol L^{-1}).

k_1 (s^{-1})	k_2 (s^{-1})	k_3 (s^{-1})	D_m (L mol^{-1} s^{-1})	c_{H+} (Mol L^{-1})
$3 * 10^{-4}$	$2 * 10^{-5}$	$4 * 10^{-2}$	10^3	10^{-4}

Table 8.1: Steady state degradation model Parameters

The velocity of the Ostwald ripening reaction can be calculated using (8.15). Ostwald ripening removes Pt atoms from small particles and deposits them on larger particles. This means that this equation can have a positive or a negative result for a particle.

$$v_4(r_{i,j}) = 4\pi D_m C_{\mathrm{Pt}} l_c \left(\frac{r_{i,j-1}}{\bar{r}_j} - 1 \right) \tag{8.15}$$

With the following parameters:

D_m Diffusion coefficient for Pt (tuning parameter) [m^2 s^{-1}].

C_{Pt} Solubility of Pt (10^{-6} Mol L^{-1}) [46].

l_c Capillary length (material constant), taken as 1 nm. [47].

$\bar{r}_j$ Average particle radius at time step j [m].

As mentioned before, the model starts of with an initial particle radius distribution with M particles (M = 140000 is used in this case). The number of Pt atoms in each particle is calculated using the radius. Then, the iterative process starts, the reaction velocities are calculated based on the particle radius and the PtO coverage. The number of Pt and PtO molecules in each particle are updated and a new radius is calculated for every particle. This is repeated until the end time is reached. Then, the final PRD and ECSA can be calculated.

8.2. Model parameters

To use the steady state model, several parameters must be chosen. There is one tuning parameter for every reaction speed equation, the equilibrium rate constants of Reactions 8.2, 8.3 and 8.4 (k_1, k_2 and k_3) and the platinum diffusion coefficient (D_m). They are chosen based on a verification experiment referenced in Ao et al. The initial particle distribution radius is taken from the same verification case [48], a lognormal distribution with $\mu = -20.5$ m and $\sigma = 0.42$ m. The probability density function of a lognormal distrubution is (8.16). Additionally, the concentration of H^+ at the electrode needs to be provided. Because it is very difficult to measure the pH inside a fuel cell, the pH at the outlet of a fuel cell is used [49]. The parameters can be found in Table 8.1.

$$\frac{1}{x\sigma\sqrt{2\pi}} \exp\left(-\frac{(\ln x - \mu)^2}{2\sigma^2} \right) \tag{8.16}$$

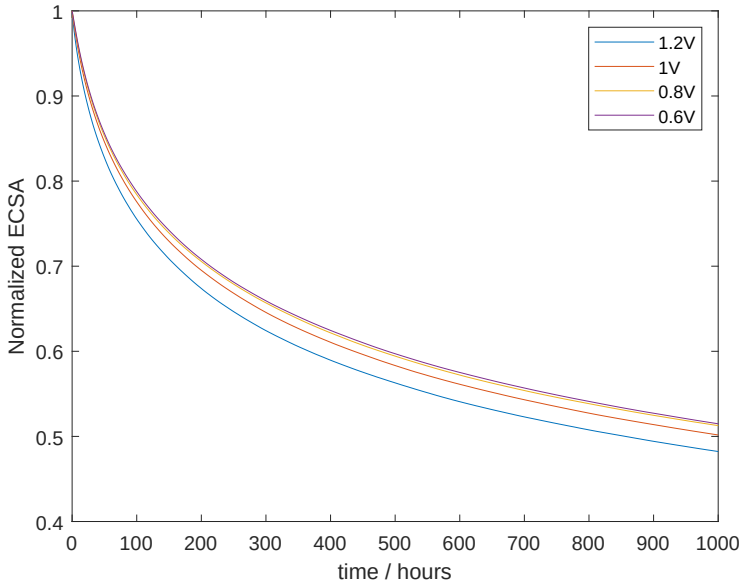

Figure 8.1: Steady state degradation for different FC voltages

8.3. Results

The most important information from the steady state degradation model can be found in Figure 8.1. The different ECSA degradation curves associated with different fuel cell voltages. It can be seen that increasing the voltage accelerates the catalyst decay.

The loss of catalyst surface lowers the fuel cell voltage, as can be seen in (8.17) from Wang et al. [50] (where $ECSA_t$ is the current ECSA and $ECSA_0$ is the original). A lower fuel cell voltage at a given leads to a decrease in maximum power and in the efficiency of the fuel cell. The End-Of-Life of a fuel cell is often defined as a voltage drop of 10%. When the fuel cell delivers half of its maximum power, the voltage is around 0.7V. Using this value and (8.17) it can be calculated that the ECSA would need to drop to 18% of its original value to reach the 10% voltage drop. It should be noted that in practice, other degradation mechanisms also contribute to the fuel cell voltage drop, which would reach the 10% drop level earlier.

$$\Delta V_{\text{activation}} = \frac{RT}{2\alpha F}\left(\ln\left(\frac{I}{I_0}\right) - \ln\left(\frac{ECSA_t}{ECSA_0}\right)\right) \tag{8.17}$$

The steady state degradation model can be used to just find the ECSA degradation, but there is additional information about the catalyst that can be extracted.

In Figure 8.2 it can be seen that the number of catalyst particles dramatically falls during the first few hundred hours of constant load. After a 1000 hours it has dropped to just over 10% of the original amount of particles.

Related to this is Figure 8.3, a comparison between the particle radius distributions over time. There it also can be seen that the total number of particles decreases, but also that there is a shift in the radius distribution towards larger particles.

This can be explained by the different catalyst degradation mechanisms. The platinum dissolution reactions remove platinum from all the particles, initially shrinking all particles. Two factors are responsible for the shift towards larger particles. Firstly,

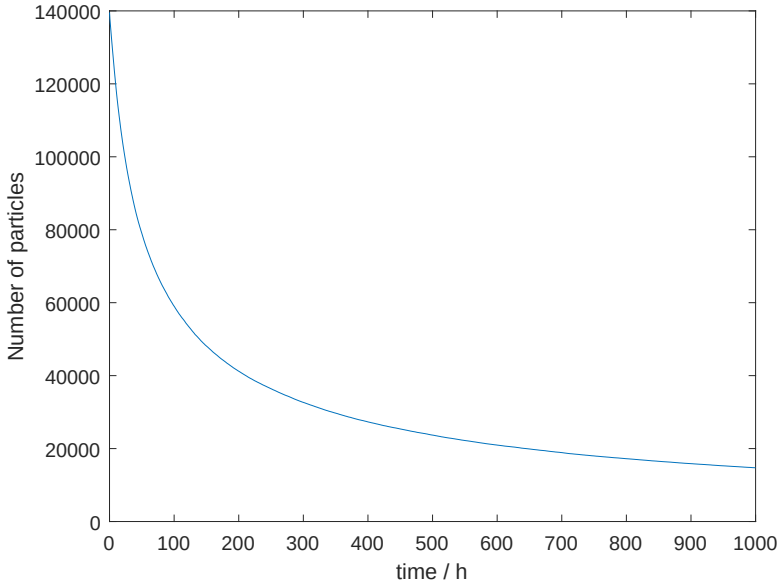

Figure 8.2: Number of Pt particles over time while exposed to steady state degradation at 0.8V at 333K.

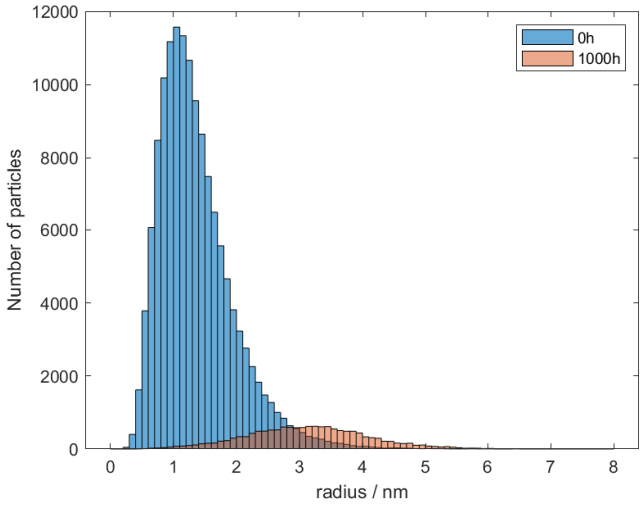

Figure 8.3: Comparison between histogram of particle radius between 0h and 1000h steady state degradation at 0.8V and 333K.

the dissolution reaction speeds are higher for smaller particles. Additionally, Ostwald ripening dissolves the small particles while adding Pt atoms to the larger particles.

8.4. Conclusion

In this chapter, the steady state degradation model was introduced. It is based on the catalyst transformation model from Ao et al. [44]. A large number of catalyst particles is simulated. For every time step, the influence of the electrochemical dissolution, chemical dissolution and Ostwald ripening degradation mechanisms is calculated for every individual particle. The oxide layer that can form at the surface of Pt particles is also taken into account. The model shows that higher fuel cell potential leads to faster ECSA degradation. The model also gives information about the size distribution of the catalyst particles. It clearly shows that the small particles dissolve and that some particles grow, shifting the distribution towards larger particle sizes. The results also show that the main way to influence the steady state degradation is through the fuel cell voltage. The main way to keep the fuel cell voltage low is to always require a minimum level of load. This something that needs to be considered during the design of the entire system the fuel cell is integrated into.

9

Current ripple degradation model

In this chapter, the modeling of the catalyst degradation due to current ripple degradation is discussed. The model is based on experimental data. The experimental results are combined with a model of the impedance of a fuel cell. This results in a model that relates the ripple amplitude, ripple frequency to the ECSA degradation over time.

9.1. Fuel cell impedance model

The steady state behavior of a fuel cell can be described using a number of equations that model the open circuit voltage and the activation losses. These models can predict the polarization curve of a fuel cell (stack), the maximum power output, the efficiency and heat and water production based on the hydrogen and air intake and a number of fuel cell specific parameters.

The reversible OCV can be calculated using the Gibbs free energy as shown in Section 2.6 in (2.3). The (partial) pressure of the reactants and the state of the produced water influence the Gibbs free energy. The Nernst equation (9.1) takes these factors into account (in this case it is assumed that the water that is produced is in the liquid phase).

$$E_{th} = E^0 + \frac{RT}{2F} \ln\left(P_{H_2} * \sqrt{P_{O_2}}\right) \tag{9.1}$$

Where E^0 is the standard potential at a pressure of 1 bar, R is the ideal gas constant, F is the Faraday constant, T is the temperature, and the partial pressures of hydrogen and oxygen are denoted by P_{H_2} and P_{O_2}.

The cell voltage is the the reversible OCV minus the different polarization losses, as stated in (9.2).

$$V_{\text{cell}} = E_{th} - \Delta V_{\text{activation}} - \Delta V_{\text{ohm}} - \left|\Delta V_{\text{transport}}\right| \tag{9.2}$$

The Tafel equation (9.3) gives the activation overvoltage of an electrochemical reaction as a function of the current. The constants in front of the logarithm are specific for a hydrogen fuel cell. The α is the charge transfer coefficient, it will be between 0.1 and 0.5 in most cases [1]. The exchange current density is represented by I_0, it is a measure of the activity at the electrode surface.

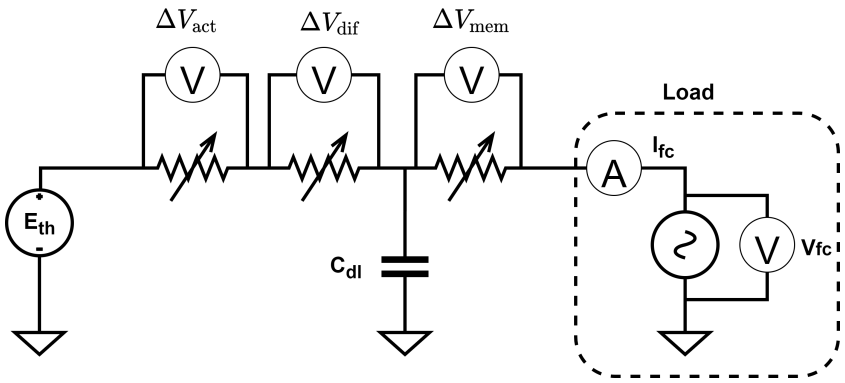

Figure 9.1: Fuel cell impedance model circuit. The polarizations are modeled as variable resistors.

$$\Delta V_{\text{activation}} = \frac{RT}{2\alpha F} \ln\left(\frac{I}{I_0}\right) \tag{9.3}$$

The transport losses can be calculated using (9.4).

$$\Delta V_{\text{transport}} = \frac{RT}{2\beta_* F} \ln\left(1 - \frac{I}{I_{\text{lim}}}\right) \tag{9.4}$$

Where β_* is a tuning parameter and I_{lim} is the maximum current that can be sustained by the transport of reactants to the electrodes by diffusion. It is assumed to be 2 A.cm^{-2}, the fuel cell surface area is 200cm^2, giving a limit of 400 A.

The conduction overvoltage is modeled as the membrane resistance, (9.5).

$$R_{\text{mem}} = \frac{l}{\sigma S} \tag{9.5}$$

Where l is the thickness of the membrane in cm, and S is the fuel cell area in cm^2. σ is the conductivity of the membrane, Mennola [51] gives (9.6) to calculate it.

$$\sigma = (0.005139\lambda_m - 0.00326) \exp\left(1268\left(\frac{1}{300} - \frac{1}{T}\right)\right) \tag{9.6}$$

Which calculates the conductivity using the hydration level λ_m and the temperature.

When comparing the modeled polarizations to those in Section 2.7, it can be noticed that the fuel crossover losses are missing. Because those only really influence the behavior of the fuel cell at OCV, they can be neglected if a minimum current of a couple of mA's is enforced.

The dynamic behavior of the fuel cell is modeled using the the method shown by Fontes et al. [7]. The polarizations are combined with the double layer capacitance using the circuit shown in Figure 9.1. The polarizations are converted to a (variable resistance) based on the applied current and the temperature. This circuit is implemented in Simulink, which can be seen in Figure 9.2.

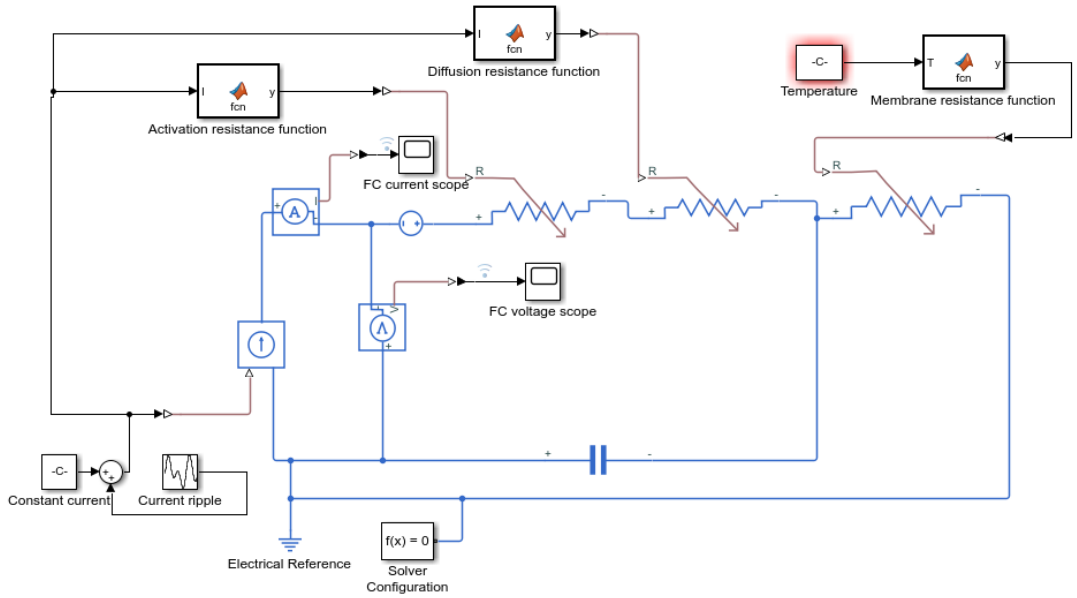

Figure 9.2: Matlab implementation of impedance model. The current ripple shape is created in the bottom left, it is then used to created the current ripple in the circuit and to calculate the resistances.

α	I_0	β	I_{lim}	λ_{m}
0.34	0.001 A	0.26	400 A	38.8

Table 9.1: Impedance model Parameters

9.1.1. Parameter estimation

The parameters in the previous equations can be obtained using two fuel cell characterization techniques, a polarization curve and an EIS. Firstly, a least squares optimization method is used to minimize the difference between the fuel cell voltages from the polarization curve and those that are calculated using (9.2). The characterization was done at a temperature (T) of 63°C and gas pressures $P_{H_2} = 1$ bar and $P_{O_2} = 0.21$ bar .

The model parameters can be found in Table 9.1. The model accurately represents the steady state behavior of the fuel cell, as can be seen in Figure 9.3.

The EIS is used to obtain the membrane resistance, by taking the real part of impedance where the imaginary part of the resistance equals zero (at the highest frequencies). The EIS of a stack of five NedStack fuel cells can be found in Figure 9.4. When the left side of the EIS curves is extrapolated, it results in a membrane resistance of 350 µΩ. S is 200 cm^2, l is taken as 0.02 cm. When this is combined with Equations 9.5 and 9.6, $\lambda_m = 38.8$ can be found. C_{dl} can also be found using the EIS curve, by estimating the location of the 'knee' of the curve and using (9.7). The activation resistance is the distance between the two intersections of the EIS curve with the real axis.

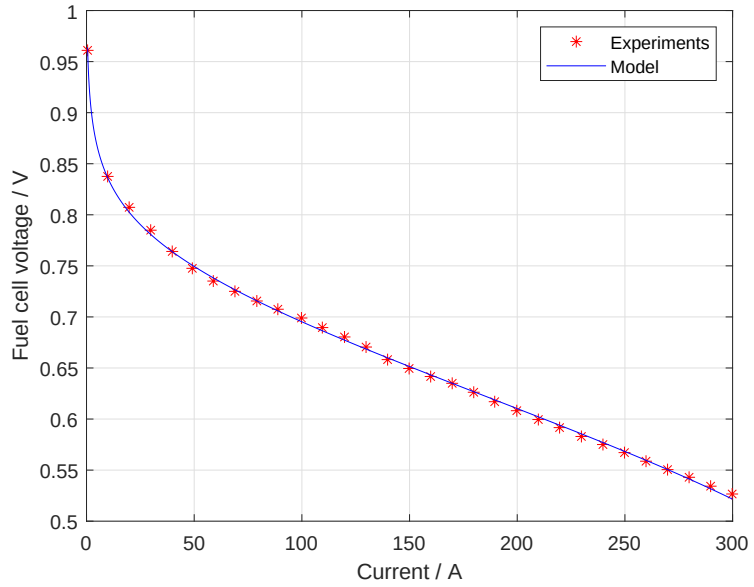

Figure 9.3: Fuel cell experimental and modeled polarization curves.

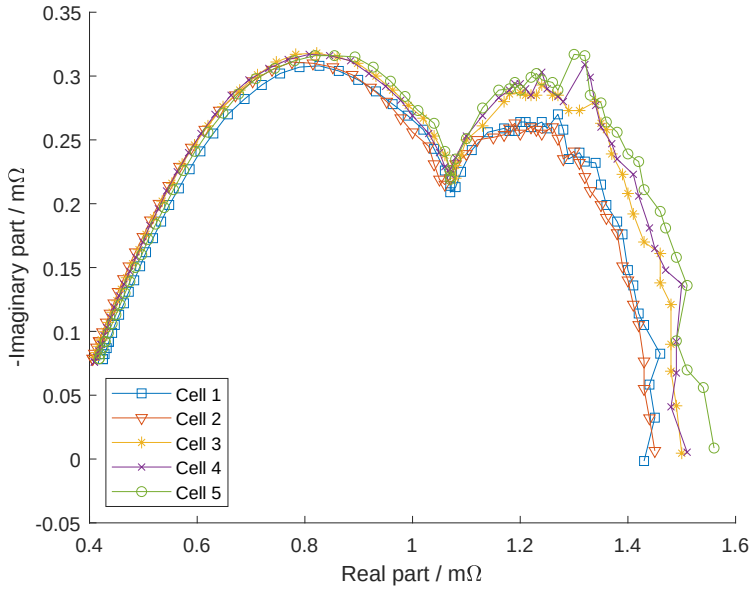

Figure 9.4: EIS of the five fuel cells

R_{act}	R_{mem}	C_{dl}
1.14 mΩ	350 µΩ	10 F

Table 9.2: Impedance model Parameters identified using EIS

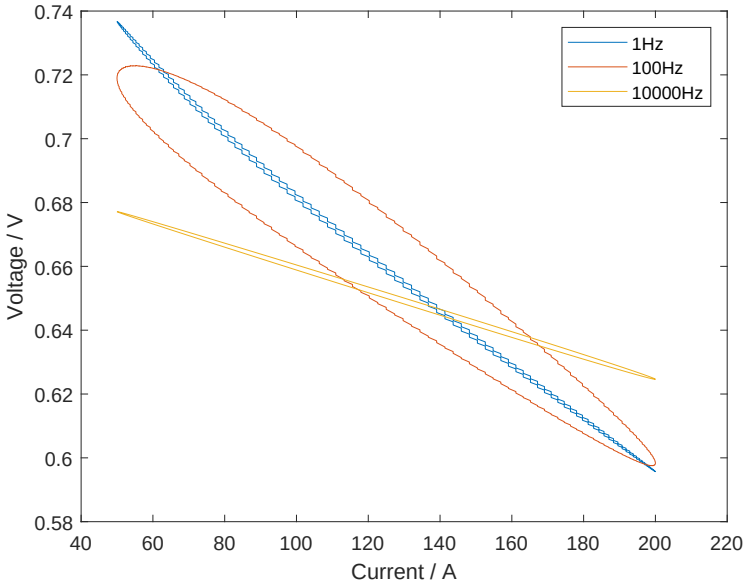

Figure 9.5: Voltage response to current ripples with different frequencies.

$$C_{dl} = \frac{1}{2\pi f_{\text{knee}} R_{\text{act}}} \tag{9.7}$$

9.1.2. Results

The goal of the impedance model is to calculate the voltage response to current ripple. Due to the double layer capacitance, the ripple frequency has a significant influence on the resulting voltage ripple. An example can be seen in Figure 9.5, where the voltage response to sinusoidal current ripples of 125±75A with 1Hz, 100Hz (low frequency current ripple) and 10000Hz (high frequency current ripple) are compared. It shows that the high frequency ripple results in significantly smaller voltage ripple. The peak-to-peak values of the voltage response can be found in Table 9.3, the 10kHz current ripple results in a voltage ripple amplitude that is under half the amplitude of the lower frequencies.

In Figure 9.6, it can be seen that the voltage response to the current ripple depends on the average current of the ripple. When a ripple with the same amplitude, and frequency but with a different average current (75A±25A, 100A0±25A, 125A±25A etc. at 100Hz in this case) is applied to the fuel cell, the higher the average current, the higher smaller the voltage response. The difference between the smallest and the largest ripple size is about 10%. This is most likely due to the IV-characteristics of the fuel cell, when looking at the polarization curve (Figure 9.3) it can be seen that the curve is steeper where the current is lower.

f_{ripple}	1Hz	100Hz	10000Hz
ΔV	0.14V	0.12V	0.053V

Table 9.3:]
Peak-to-peak voltage ripple associated with 125A±75A sinusoidal current ripple with different frequencies.

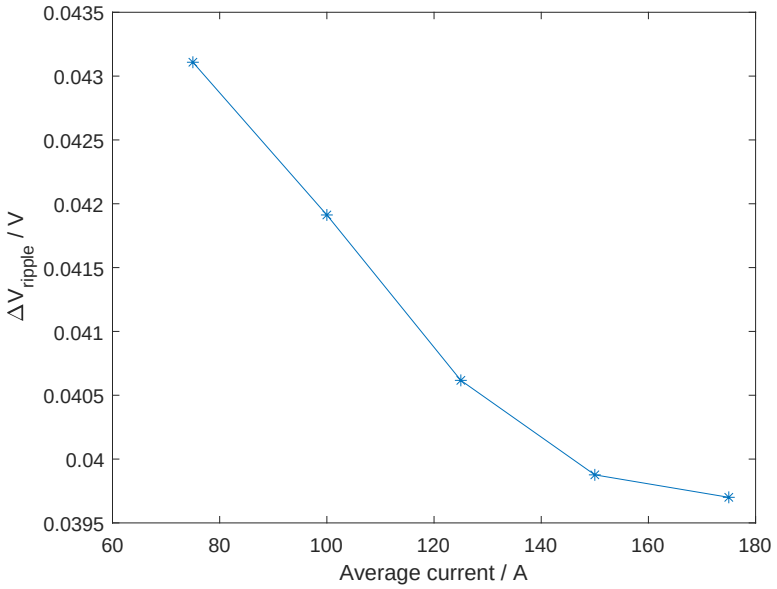

Figure 9.6: Peak-to-peak voltage response to current ripple with different average current. Ripple amplitude: 25A, ripple frequency: 100Hz

9.2. Current ripple degradation model

The voltage ripple is converted to the relative ECSA degradation rate by multiplying it with a base ECSA degradation rate (9.8). This base ECSA degradation rate is based on experimental data, and has the unit $V^{-1}h^{-1}$.

$$\text{ECSA degradation rate} = \Delta V_{\text{ripple}} * \text{base ECSA degradation rate} \tag{9.8}$$

9.3. Conclusion

In this chapter, the current ripple degradation model were introduced. It is based on the PEM fuel cell impedance model introduced by Fontes et al. [7]. The model consists of a equivalent electrical circuit with variable resistors that follow the basic PEMFC polarization equations. The double layer capacitance is emulated by a capacitor to accurately imitate the dynamic behaviour of the fuel cell. The parameters of the model were obtained using the polarization curve and an EIS plot. The results of the impedance model are in agreement with the general behaviour of fuel cells. Ripple with a low frequency (<100Hz) gives the largest voltage fluctuations, and ripple with a frequency around 100hz results in hysteresis due to the capacitor-resistor pair in the equivalent circuit. The impedance model can be used to extrapolate the data obtained by a current ripple degradation experiment to different ripple shapes. This experiment would need to compare ECSA degradation of a fuel cell over time, when it is subjected to current ripple, to the degradation of a fuel cell when it is subjected to a constant load. The ECSA can be measured using cyclic voltammetry. The final result of the experiment is a relative ECSA degradation rate in $V^{-1}h^{-1}$.

10 Results

This chapter discusses the results that are obtained using the steady state degradation model and the current ripple degradation model. The model that has been developed still needs to be validated using experiments. An experiment that should be performed to greatly increase the accuracy and effectiveness of both models is also proposed.

The output from steady state degradation model and the ripple degradation model are relative ECSA decreases over time. For example, after 100 hours steady state degradation resulted in an ECSA decrease of 10% and ripple degradation resulted in an ECSA decrease of 11%. These factors are then simply added up towards a total ECSA degradation (21%).

10.1. Comparison between degradation types

The model needs the base ECSA degradation rate, which is experimentally determined to function correctly. Unfortunately, there is a general lack of current ripple induced ECSA degradation data in literature. Kim et al. does report the increase in the EIS activation resistance (3.9mΩto 7.9mΩ) after 100h of a 100Hz current ripple of 20A±10A (resulting in a voltage ripple of 0.1V). The activation resistance is a function of the ECSA and the surface concentrations of the reactants. For convenience, it is assumed that it scales linearly with the ECSA. This leads to a base relative ECSA degradation rate of 0.049 $V^{-1}h^{-1}$.

The ripple degradation model works by multiplying the relative ECSA degradation rate with the peak-to-peak of the voltage ripple.

With this placeholder ripple ECSA degradation rate, it can be shown how the total model would work. The hypothetical case is current ripple of 20% around an average current of 100A with a frequency of 20kHz, this could for example be caused by a boost converter. This data is fed into the impedance model, which returns an average voltage of 0.7V and a peak-to-peak value of 0.014V. The 0.7V is used the voltage input for the steady state degradation module. The 0.014V leads to a ECSA degradation rate of $686 * 10^{-6} h^{-1}$. The results can be found in Figure 10.1, which shows the contributions of both degradation mechanism to the total ECSA degradation over time. The End of Live state of 18% remaining ECSA is reached after after 582h.

This kind of data can be used in the design process of fuel cell systems. The lifetime of a fuel cell is an important factor in most fuel cell applications. This model

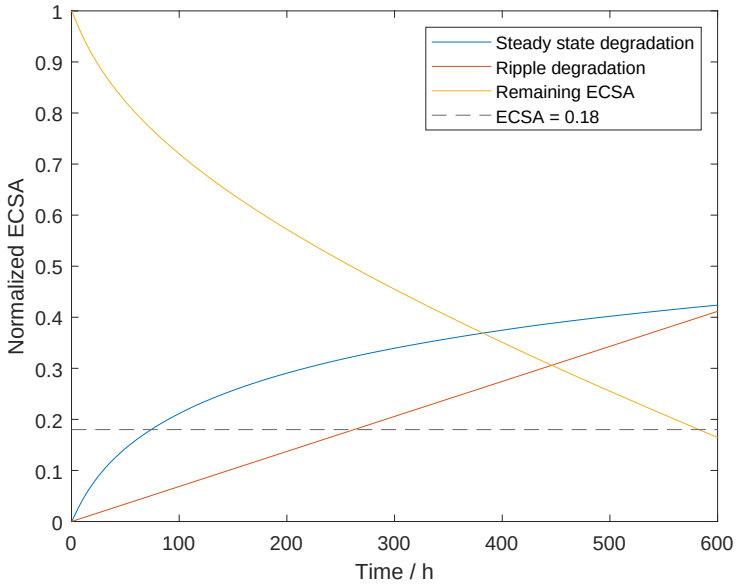

Figure 10.1: ECSA degradation for 20% ripple at 100A. The contributions of steady state and ripple degradation are shown. The dashed line represents the End of Live criterium.

is a way to quantify the influence of the different power electronics design options (related to current ripple) on the catalyst lifetime. In Figure 10.2, it is shown how the ripple frequency can influence the ECSA degradation rate. The difference between high frequency current ripple (1kHz and 20kHz) and the low frequency current ripple (100Hz) is very clear. The low frequency current ripple reaches end of life in half the time as the higher frequencies. It should also be noted how close the results for 1kHz and 20kHz are, there is nothing to be won by increasing switching frequencies with regard to degradation.

Figure 10.3 shows the influence of the ripple amplitude on the ECSA degradation, it can be seen that decreasing the ripple amplitude increases the predicted lifetime.

10.2. Current ripple degradation experiment

The translation from the output of the impedance model to the degradation rate is based on experimental data. But these current ripple catalyst degradation experiments have not yet been performed. Fuel cell degradation experiments can take a very long time since the degradation occurs over the entire lifetime of a fuel cell, which could be thousands of hours. To combat this, fuel cell degradation experiments often use conditions that accelerate the degradation, high temperatures, high pressure, low relative humidity, extreme load profiles etc. depending on what degradation mechanisms is investigated. In the case of current ripple, the experiment parameters that will make sure that degradation will occur the quickest (while not introducing additional catalyst degradation stressors) are a low frequency, high amplitude current ripple.

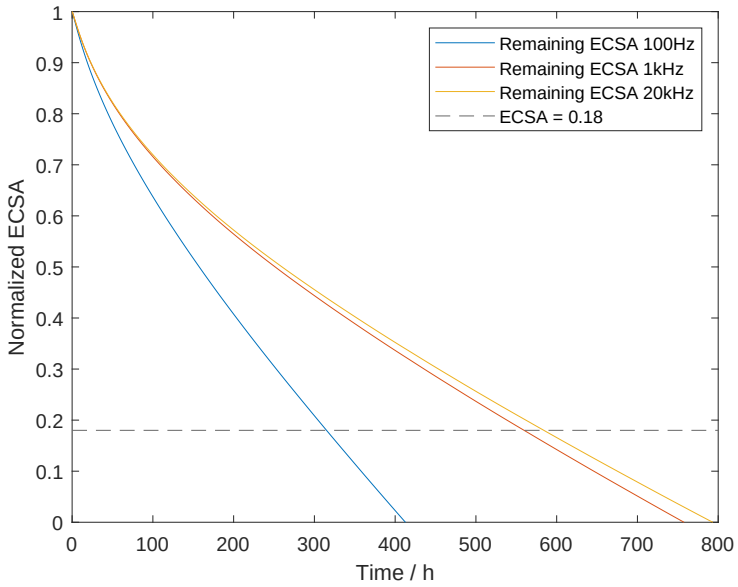

Figure 10.2: Comparison of ECSA degradation for 20% ripple at 100A for 100Hz, 1000Hz and 20kHz. The dashed line represents the End of Live criterium.

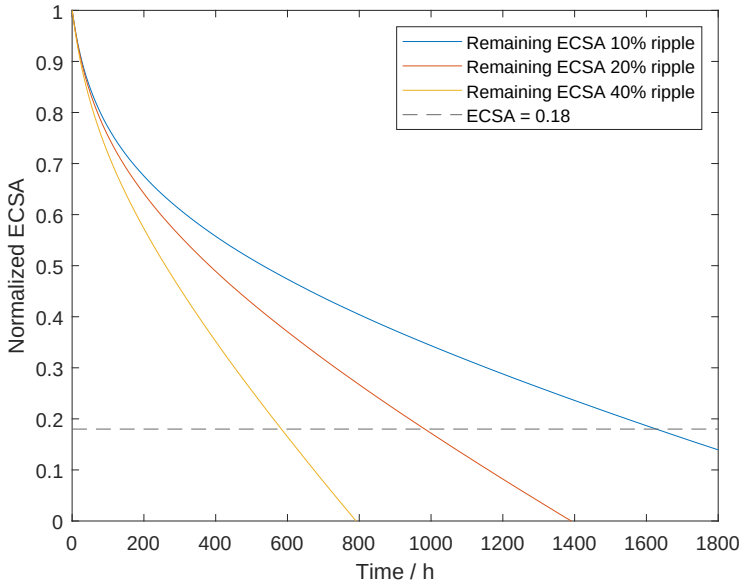

Figure 10.3: Comparison of ECSA degradation for 20kHz ripple at 100A with 10%, 20% and 40% ripple. The contributions of steady state and ripple degradation are shown. The dashed line represents the End of Live criterium.

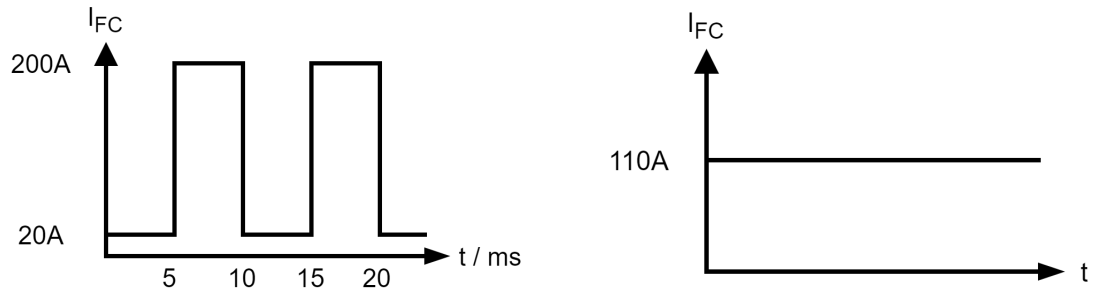

(a) Current ripple shape during experiment

(b) Reference load during experiment

Figure 10.4: Applied loads during ECSA degradation experiment

10.2.1. Methodology

The goal of the experiment is to find the relationship between current ripple that is applied to the fuel cell stack and the ECSA degradation over time. Ideally different ripple shapes (frequency, amplitude, average current) are tested, but as mentioned before, fuel cell degradation experiments take a long time and can be expensive.

The most damaging current ripple that can be chosen for a NedStack test short stack consists of a square wave between 20A and 200A at 100Hz, see Figure 10.4a. This ripple shape was chosen because it has the biggest possible amplitude, while staying well away from the fuel cell current associated with the OCV on one hand, and the current limit on the other.

To distinguish the ECSA degradation caused by current ripple from the ECSA degradation that would be caused by a constant current, a reference degradation test is performed. The average of the current ripple (110A) is taken as the load during the reference test (Figure 10.4b).

The testing procedure would be as follows:

1. Initial characterization
2. Reference degradation test (1 week)
3. Characterization
4. Ripple degradation test (1 week)
5. Final characterization

The ECSA is measured using cyclic voltammetry, a technique that works by applying a voltage to the fuel cell and recording the associated current flowing through the fuel cell. The general idea is that the fuel cell potential is cycles through a voltage range in which the electron transfer reactions occur at the electrode surface. The number of reactive sites can then be obtained using the total charge required for monolayer adsorption or desorption of hydrogen on the platinum particles. In Figure 10.5, the result of a cyclic voltammetry experiment, a schematic voltammetrogram is shown. To determine the ECSA of a fuel cell, the surface of the shaded area needs to be calculated, to get the charge necessary for monolayer hydrogen adsorption that was mentioned before. This area is delimited at the top by the current associated with a

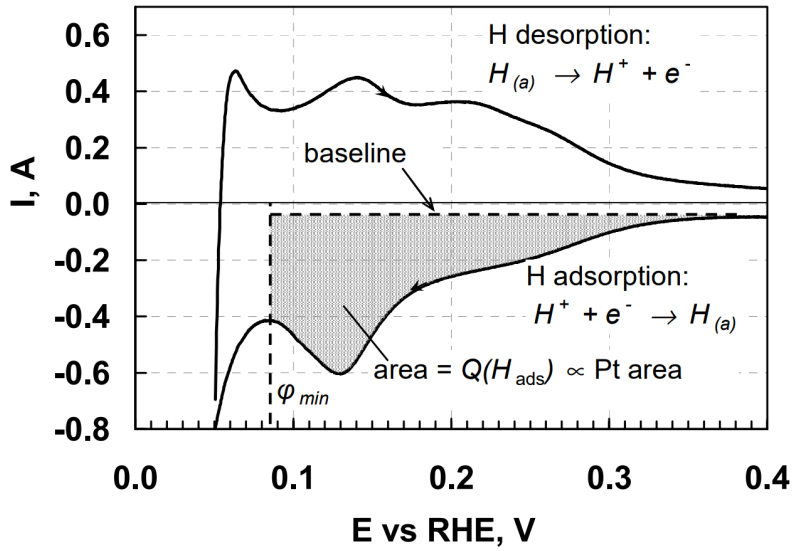

Figure 10.5: Schematic cyclic voltammetrogram of fuel cell. The surface of the shaded area is the charge associated with hydrogen adsorption on the catalyst particles.

potential of 0.4V, and on the left side by the vertical line through the the local maximum at the bottom left. To subsequently convert the charge into the ECSA, the ratio 210 µC cm^{-2}(pt) is used. This ratio is commonly used for carbon-supported platinum catalysts.

10.3. Conclusion

in this chapter the results from the steady state degradation model and the current ripple degradation model were combined. Additionally, the methodology for an experiment that investigates catalyst degradation due to current ripple was introduced. Such an experiment is necessary to use the catalyst degradation models to their full potential.

11

Conclusion & Recommendations

11.1. Conclusion

In part II, the modeling methodology for the steady state degradation model and the ripple degradation model has been discussed. To investigate the influence of current ripple on the catalyst of a proton exchange fuel cell, a method has been proposed to predict ECSA degradation based on the voltage ripple that is associated with the current ripple. When a load introduces current ripple into a fuel cell there are three important parameters: the average current, the ripple amplitude and the ripple frequency. The first model that has been implemented describes the transformation of the Platinum catalyst particles due to the corrosive conditions inside the fuel cell due to the acidity, electric potential and temperature. The second model calculates the voltage ripple associated with the current ripple and uses this to predict the catalyst degradation rate due to the ripple. The overview of the models can be seen in Figure 11.1.

The models were designed to fulfill the objective of the follow-up research:

Develop a model of the current ripple induced catalyst degradation in a proton exchange membrane fuel cell.

In Chapter 8, the degradation of a fuel cell catalyst under a constant load is modeled. A catalyst transformation model was implemented to simulate the state of Pt catalyst particles over time. Reaction pathways for electrochemical dissolution, chemical dissolution and Ostwald ripening are implemented as degradation mechanisms.

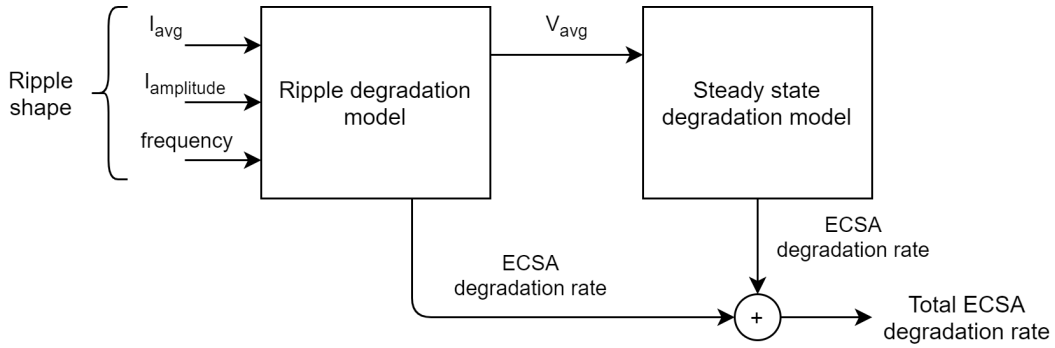

Figure 11.1: Schematic overview of model structure (reproduced from Figure 7.3)

The speed of the reactions depends on the fuel cell voltage, the temperature and the particle size. The model showed that the best way to combat steady state degradation is to lower the fuel cell voltage. This needs to be addressed during the design of the power system the fuel cells are integrated into, since it requires a minimum that is always present for the fuel cell stack.

Chapter 9 described the approach of formulating the ripple degradation model. It uses a fuel cell impedance model to extrapolate experimental ripple degradation data to different ripple shapes (ripple amplitude, average current and frequency). Due to the incremental nature of fuel cell degradation under normal conditions, experiments investigating this take a long time, making it not feasible to compare the degradation of different ripple shapes. The impedance model consists of an equivalent electrical circuit, where the activation resistance, diffusion resistance and the membrane resistance are calculated as a function of the fuel cell current. The impedance model is used to calculate the voltage response to the current ripple, the final result being the peak-to-peak value of the voltage ripple. This value is then used to scale the catalyst degradation rate from the experimental results when the ripple shape is different from the ripple shape used in the experiment. The model shows that current ripple with a higher frequency results in a smaller peak-to-peak voltage response. This is due to the double layer capacitance, filtering out (part of) the high frequency signal. The average current has a small influence on the voltage response, it gets slightly smaller when the average current rises.

The model introduced in this thesis can be used to calculate the influence of current ripple on catalyst degradation, and subsequently its influence on the lifetime of the fuel cell. However, the model still needs to be verified and it can not yet give answers about the magnitude of catalyst degradation due to current ripple, and how it compares to other types of degradation. Additionally, due to it being built around extrapolating experimental data, the model can not really give new insights into fuel cell degradation due to current ripple.

11.2. Recommendations

There are many questions that remain on the topic of the influence of current ripple on PEM fuel cell degradation. Additionally there are recommendations to improve the introduced model.

- To be able fully to use both models, experimental data is needed. The experiment should separate the ECSA degradation due to current ripple from the ECSA damage due to the average load. This can be done by doing two different test, a ripple test and a constant load test (with the applied current being the average current of the ripple). The ripple degradation rate is used as an input in the ripple degradation model. The reference test can be used to tune the steady state degradation model.

- To validate the ripple degradation model (and improve its accuracy), it is desired that the assumptions are experimentally verified. The model assumes that the ECSA degradation scales linearly with the voltage ripple, that the ripple frequency does not directly influence the the ECSA degradation rate and that the

ECSA degradation due to ripple stays constant over time. These are hypotheses that would require a significant amount of experimental work to investigate, but they are important for predicting the damage current ripple does to a fuel cell catalyst.

- In the literature review it was concluded that there little insight into the catalyst degradation mechanisms that are associated with current ripple. More qualitative research is needed. To investigate this further, more long-term degradation experiments are necessary. Up until this point, electrical methods (electrical impedance spectroscopy and cyclic voltammetry) have been applied when researching this topic. Perhaps the step towards in-situ measurements needs to be made.
- It could be interesting to incorporate the model into the design process of fuel cell BoP power electronics, maybe in a simplified version to make it easier to implement in design environments.
- Aside from the catalyst degradation, the influence of current ripple on the other components of a fuel cell also deserves a closer look. In literature it was found that current ripple can have an influence on the water management. There are also clues that point towards the membrane as an interesting subject with regard to high frequency current ripple (>10kHz). Purely theoretically, because the membrane is the main source of resistance for high frequency signals, and experimentally.

Bibliography

[1] James Larminie, Andrew Dicks, and Maurice S McDonald. *Fuel cell systems explained*. Vol. 2. J. Wiley Chichester, UK, 2003.

[2] Toyota. *2021 Toyota Mirai Fuel Cell Vehicle | Innovation is Power*. en. URL: https://www.toyota.com/mirai/ (visited on 05/18/2021).

[3] Honda. *2021 Honda Clarity Fuel Cell – Hydrogen-Powered Car | Honda*. en. 2021. URL: https://automobiles.honda.com:443/clarity-fuel-cell (visited on 05/18/2021).

[4] Leslie Eudy and Matthew Post. "Fuel Cell Buses in U.S. Transit Fleets: Current Status 2020". en. In: *Renewable Energy* (2021), p. 57.

[5] Fuelcellbuses EU. *The JIVE projects celebrate a milestone 200 buses have been ordered!.pdf*. Sept. 2020. URL: https://www.fuelcellbuses.eu/sites/default/files/documents/The%20JIVE%20projects%20celebrate%20a%20milestone%20200%20buses%20have%20been%20ordered%21.pdf (visited on 06/23/2021).

[6] *Nemo H2: rondvaart op waterstof*. Tech. rep. DEMO06005. Agentschap NL, July 2011. URL: https://www.rvo.nl/sites/default/files/rvo_website_content/EOS/DEMO06005.pdf (visited on 05/18/2021).

[7] Guillaume Fontes et al. "Interactions between fuel cells and power converters: Influence of current harmonics on a fuel cell stack". In: *IEEE Transactions on Power Electronics* 22.2 (2007). Publisher: IEEE, pp. 670–678.

[8] Kenneth A Mauritz and Robert B Moore. "State of understanding of Nafion". In: *Chemical reviews* 104.10 (2004). Publisher: ACS Publications, pp. 4535–4586.

[9] FA De Bruijn, VAT Dam, and GJM Janssen. "Durability and degradation issues of PEM fuel cell components". In: *Fuel cells* 8.1 (2008). Publisher: Wiley Online Library, pp. 3–22.

[10] Cabot. *VULCAN® XC72*. URL: https://chem-on.com.sg/image/catalog/product_catalog/TDS%20-%20VULCAN%20XC72.pdf (visited on 04/02/2021).

[11] Abid Rabbani and Masoud Rokni. "Dynamic performance of a PEM fuel cell system". PhD Thesis. Ph. D. Thesis, Technical University of Denmark, 2013.

[12] Jong-Hoon Kim et al. "An experimental analysis of the ripple current applied variable frequency characteristic in a polymer electrolyte membrane fuel cell". In: *Journal of Power Electronics* 11.1 (2011), pp. 82–89.

[13] Yuxi Song et al. "Review on current research of materials, fabrication and application for bipolar plate in proton exchange membrane fuel cell". In: *International Journal of Hydrogen Energy* 45.54 (2020). Publisher: Elsevier, pp. 29832–29847.

[14] Liangfei Xu et al. “Interactions between a polymer electrolyte membrane fuel cell and boost converter utilizing a multiscale model”. In: *Journal of Power Sources* 395 (2018). Publisher: Elsevier, pp. 237–250.

[15] Fei Gao et al. “Fuel Cell System”. In: *Power Electronics for Renewable and Distributed Energy Systems: A Sourcebook of Topologies, Control and Integration*. Ed. by Sudipta Chakraborty, Marcelo G. Simões, and William E. Kramer. London: Springer London, 2013, pp. 185–234. ISBN: 978-1-4471-5104-3. DOI: 10.1007/978-1-4471-5104-3_6. URL: https://doi.org/10.1007/978-1-4471-5104-3_6.

[16] Yu Jin Song. “Analysis and design of high frequency link power conversion systems for fuel cell power conditioning”. PhD Thesis. Texas A&M University, 2005.

[17] U.S. DRIVE partnership. *Fuel Cell Technical Team Roadmap*. Tech. rep. 2017. URL: https://www.energy.gov/sites/default/files/2017/11/f46/FCTT_Roadmap_Nov_2017_FINAL.pdf (visited on 04/16/2021).

[18] Hongtao Zhang et al. “Enhancing fuel cell durability for fuel cell plug-in hybrid electric vehicles through strategic power management”. In: *Applied Energy* 241 (2019). Publisher: Elsevier, pp. 483–490.

[19] Yunjin Ao et al. “Lifetime prediction for proton exchange membrane fuel cell under real driving cycles based on platinum particle dissolve model”. In: *International Journal of Hydrogen Energy* 45.56 (2020). Publisher: Elsevier, pp. 32388–32401.

[20] Thomas Jahnke et al. “Performance and degradation of Proton Exchange Membrane Fuel Cells: State of the art in modeling from atomistic to system scale”. In: *Journal of Power Sources* 304 (2016). Publisher: Elsevier, pp. 207–233.

[21] Y Shao-Horn et al. “Instability of supported platinum nanoparticles in low-temperature fuel cells”. In: *Topics in Catalysis* 46.3 (2007). Publisher: Springer, pp. 285–305.

[22] Serhiy Cherevko, Nadiia Kulyk, and Karl JJ Mayrhofer. “Durability of platinum-based fuel cell electrocatalysts: Dissolution of bulk and nanoscale platinum”. In: *Nano energy* 29 (2016). Publisher: Elsevier, pp. 275–298.

[23] Jinfeng Wu et al. “A review of PEM fuel cell durability: Degradation mechanisms and mitigation strategies”. In: *Journal of Power Sources* 184.1 (2008). Publisher: Elsevier, pp. 104–119.

[24] Yuyan Shao, Geping Yin, and Yunzhi Gao. “Understanding and approaches for the durability issues of Pt-based catalysts for PEM fuel cell”. In: *Journal of Power Sources* 171.2 (2007). Publisher: Elsevier, pp. 558–566.

[25] Shimshon Gottesfeld and Judith Pafford. “A new approach to the problem of carbon monoxide poisoning in fuel cells operating at low temperatures”. In: *J. Electrochem. Soc* 135.10 (1988). Publisher: Citeseer, pp. 2651–2652.

[26] Fumiya Hiraoka, Koichi Matsuzawa, and Shigenori Mitsushima. “Degradation of Pt/C under various potential cycling patterns”. In: *Electrocatalysis* 4.1 (2013). Publisher: Springer, pp. 10–16.

[27] LM Roen, CH Paik, and TD Jarvi. “Electrocatalytic corrosion of carbon support in PEMFC cathodes”. In: *Electrochemical and Solid State Letters* 7.1 (2003). Publisher: IOP Publishing, A19.

[28] Jan Hendrik Ohs et al. “Modeling hydrogen starvation conditions in proton-exchange membrane fuel cells”. In: *Journal of Power Sources* 196.1 (2011). Publisher: Elsevier, pp. 255–263.

[29] Jaeman Park et al. “A review of the gas diffusion layer in proton exchange membrane fuel cells: durability and degradation”. In: *Applied Energy* 155 (2015). Publisher: Elsevier, pp. 866–880.

[30] Carlos Restrepo et al. “A review of the main power electronics’ advances in order to ensure efficient operation and durability of PEMFCs”. In: *Automatika: časopis za automatiku, mjerenje, elektroniku, računarstvo i komunikacije* 53.2 (2012), pp. 184–198.

[31] Phatiphat Thounthong et al. “Fuel cell current ripple mitigation by interleaved technique for high power applications”. In: *2009 IEEE Industry Applications Society Annual Meeting*. IEEE, 2009, pp. 1–8.

[32] Rong-Jong Wai and Chun-Yu Lin. “Active low-frequency ripple control for clean-energy power-conditioning mechanism”. In: *IEEE Transactions on Industrial Electronics* 57.11 (2010). Publisher: IEEE, pp. 3780–3792.

[33] Marija Vujacic et al. “Evaluation of DC voltage ripple in three-phase PWM voltage source inverters”. In: *2017 IEEE 26th International Symposium on Industrial Electronics (ISIE)*. IEEE, 2017, pp. 711–716.

[34] Pekik Argo Dahono, Yukihiko Sato, and Teruo Kataoka. “Analysis and minimization of ripple components of input current and voltage of PWM inverters”. In: *IEEE Transactions on Industry Applications* 32.4 (1996). Publisher: IEEE, pp. 945–950.

[35] Roberto Ferrero, Mirko Marracci, and Bernardo Tellini. “Single PEM fuel cell analysis for the evaluation of current ripple effects”. In: *IEEE Transactions on Instrumentation and Measurement* 62.5 (2012). Publisher: IEEE, pp. 1058–1064.

[36] Xiaozi Yuan et al. “AC impedance technique in PEM fuel cell diagnosis—A review”. In: *International Journal of Hydrogen Energy* 32.17 (2007). Publisher: Elsevier, pp. 4365–4380.

[37] Mathias Gerard et al. “Ripple current effects on PEMFC aging test by experimental and modeling”. In: *Journal of fuel cell science and technology* 8.2 (2011). Publisher: American Society of Mechanical Engineers Digital Collection.

[38] Randall S Gemmen. “Analysis for the effect of inverter ripple current on fuel cell operating condition”. In: *J. Fluids Eng.* 125.3 (2003), pp. 576–585.

[39] Woojin Choi. “New approaches to improve the performance of the PEM based fuel cell power systems”. PhD Thesis. Texas A&M University, 2005.

[40] Yuedong Zhan et al. “Comprehensive influences measurement and analysis of power converter low frequency current ripple on PEM fuel cell”. In: *International Journal of Hydrogen Energy* 44.59 (2019). Publisher: Elsevier, pp. 31352–31359.

[41] Jonghoon Kim et al. “Impedance-based diagnosis of polymer electrolyte membrane fuel cell failures associated with a low frequency ripple current”. In: *Renewable energy* 51 (2013). Publisher: Elsevier, pp. 302–309.

[42] Bouchra Wahdame et al. “Impact of power converter current ripple on the durability of a fuel cell stack”. In: *2008 IEEE International Symposium on Industrial Electronics*. IEEE, 2008, pp. 1495–1500.

[43] Masatoshi Uno and Koji Tanaka. “Pt/C catalyst degradation in proton exchange membrane fuel cells due to high-frequency potential cycling induced by switching power converters”. In: *Journal of Power Sources* 196.23 (2011). Publisher: Elsevier, pp. 9884–9889.

[44] Yunjin Ao et al. “Proton exchange membrane fuel cell degradation model based on catalyst transformation theory”. In: *Fuel Cells* (2021). Publisher: Wiley Online Library.

[45] RD Vengrenovitch. “On the Ostwald ripening theory”. In: *Acta metallurgica* 30.6 (1982). Publisher: Elsevier, pp. 1079–1086.

[46] Ryosuke Jinnouchi et al. “First principles calculations on site-dependent dissolution potentials of supported and unsupported Pt particles”. In: *The Journal of Physical Chemistry C* 114.41 (2010). Publisher: ACS Publications, pp. 17557–17568.

[47] Yves De Smet, Luc Deriemaeker, and Robert Finsy. “A simple computer simulation of Ostwald ripening”. In: *Langmuir* 13.26 (1997). Publisher: ACS Publications, pp. 6884–6888.

[48] Yuyan Shao et al. “Durability study of Pt/ C and Pt/ CNTs catalysts under simulated PEM fuel cell conditions”. In: *Journal of the Electrochemical Society* 153.6 (2006). Publisher: IOP Publishing, A1093.

[49] J Healy et al. “Aspects of the chemical degradation of PFSA ionomers used in PEM fuel cells”. In: *Fuel cells* 5.2 (2005). Publisher: Wiley Online Library, pp. 302–308.

[50] Yongqiang Wang et al. “Power management system for a fuel cell/battery hybrid vehicle incorporating fuel cell and battery degradation”. In: *International Journal of Hydrogen Energy* 44.16 (2019). Publisher: Elsevier, pp. 8479–8492.

[51] Tuomas Mennola. “Design and experimental characterization of polymer electrolyte membrane fuel cells”. In: (2000), p. 92.

A

Scientific Research Paper

Influence of current ripple on proton exchange membrane fuel cell degradation

H.E. Wesseling, H. Polinder, J. Bruinsma, L. van Biert

Increasing the durability remains an important subject for proton exchange membrane fuel cells (PEMFC). PEMFC require power electronics to stabilize and boost the delivered power. This introduces current ripple into the fuel cell, which has been suspected to influence its degradation. In this paper, a model is developed which predicts the degradation of the PEMFC catalyst caused by current ripple. The model consists of two sub-models. The steady state degradation model predicts the decrease of the electrochemically active surface area (ECSA) due to the average current of the current ripple. It models the influence of electrochemical dissolution, chemical dissolution and Ostwald ripening on the ECSA over time. The ripple degradation model predicts the ECSA degradation as a function of the ripple amplitude and frequency, using an electrical representation of the fuel cell and experimental degradation data. The model can be used to help in the design process of power electronics that interface with fuel cells.

I. Introduction

The transition away from fossil fuel based energy production relies on the development and improvement of alternative power sources. Fuel cells produce energy without harmful emissions and could play a role in this transition towards sustainable energy. The proton exchange membrane fuel cell (PEMFC) can be used in different applications, from mobility, such as cars, buses and ships, to residential or industrial power systems [1**?** , 2]. Two barriers that still stand between PEMFC and widespread commercial adoption are the costs and the durability of the fuel cells [3].

Fuel cell degradation can occur through the decay of the catalyst, electrodes or membrane [4, 5]. The most important indicator of the health of the catalyst is the electrochemically active surface area (ECSA). A decrease in ECSA can be caused by platinum dissolution [6], platinum redisposition or detachment of platinum particles. The carbon electrodes are very stable and only degrade in case of a (local) lack of hydrogen. The membrane degrades under the influence of the mechanical forces, heat and chemical attack [4, 5]. The decay of the membrane only has a limited effect on the performance of a fuel cell during most of its lifetime, it can however, lead to failure of the fuel cell.

The voltage of fuel cells needs to be boosted and stabilized for most applications. Power electronics form the bridge between the fuel cells and the load. The power electronics introduce disturbances into the electric signal, current ripple. A distinction can be made between high frequency current ripple (>10kHz) and low frequency current ripple (100Hz - 120Hz) [7]. High frequency current ripple originates from the DC-DC conversion in the power electronics, the frequency of the ripple is directly related to the pulse width modulation (PWM) switching frequency. Low frequency current ripple is produced by a single phase inverter (DC-AC conversion). The frequency is twice the AC frequency, either 100Hz or 120Hz in most cases. Current ripple can be reduced using passive or active methods, but they add costs and complexity to the system [7, 8].

The influence of current ripple on fuel cells is a subject that has garnered academic attention. Firstly, Gemmen [9] performed simulations that indicated that the transport of oxygen to the cathode could be affected by a current ripple with a frequency of 120Hz or lower. Experiments from Choi [10] show that low frequency current ripple can reduce the efficiency and maximum power output of fuel cells by 9% for

very high ripple amplitudes, a maximum amplitude of 30% was advised to minimize power loss. Zhan et al. [11] confirmed that current ripple can result in lower fuel cell efficiency, while also finding that increasing the ripple frequency (between 50Hz and 400Hz) results in lower efficiency losses. This occurs due to the double layer capacitance phenomenon at the surface of the electrodes which filters out high frequency signals. This effect is more pronounced at higher frequencies, Fontes et al. [12] applied a current ripple with an amplitude of 100% and a frequency of 19.7kHz to a fuel cell which resulted in a voltage ripple of 6%.

Current ripple also has an effect on the degradation of fuel cells. Both low- and high frequency current ripple can cause early failure of fuel cells [11, 13]. It has also been found that low frequency current ripple causes more incremental degradation (which decreases the fuel cell voltage but does not lead to failure) than high frequency current ripple [14]. Wahdame et al. [15] reported a 10% increase in fuel cell degradation when a stack was subjected to a high frequency current ripple. Additionally, there are indications that current ripple can influence the water management inside a fuel cell [13, 16].

There is not yet a quantitative analysis of the effect of current ripple on the degradation of PEMFCs. The existing research uses experiments, which due to the length and associated costs, can only investigate a limited amount of different ripple shapes (amplitude and frequency). A prediction of the degradation that a current ripple with a certain amplitude and frequency would cause over time would be valuable for the design of the power electronics that interface with fuel cells. In this paper a model is introduced that predicts the ECSA degradation rate of a PEMFC caused by current ripple as a function of the ripple shape. The ECSA degradation is split into two parts, steady state degradation due to the average current, and ripple degradation, which is caused by the fluctuation of the current. The model consists of two sub-models, the steady state degradation model and the ripple degradation model, their respective results are added up for the total ECSA degradation.

II. Methodology

A. Assumptions

The construction of the model requires a number of assumptions:

- No spatial differences within the electrode.
- Input and output cell pressures are constant and equal.
- Gas diffusion is in steady state.
- Temperature and hydration are constant and known.
- Ripple ECSA degradation scales with voltage amplitude of the ripple.
- Ripple frequency does not directly influence ECSA degradation rates (only through its effect on the voltage amplitude).

The model is applied to a NedStack fuel cell.

B. Steady state degradation model

The mechanisms responsible for PEMFC catalyst degradation are not yet fully understood, but the main reaction products are considered to be Pt^{2+} and PtO [17]. The steady state degradation model was introduced by Ao et al. [18]. The modeled degradation mechanisms are: electrochemical dissolution (1), chemical dissolution (2) & (3), and Ostwald ripening, which is the transfer of Pt atoms from small catalyst particles to larger particles. reaction (2) leads to an PtO layer on the particles, which protects the particles from electrochemical dissolution.

$$\mathrm{Pt} \leftrightarrow \mathrm{Pt}^{2+} + 2e^- \tag{1}$$

$$\mathrm{Pt} + \mathrm{H_2O} \leftrightarrow \mathrm{PtO} + 2\mathrm{H}^+ + 2e^- \tag{2}$$

$$\mathrm{PtO} + 2\mathrm{H}^+ \leftrightarrow \mathrm{Pt}^{2+} + \mathrm{H_2O} \tag{3}$$

The model starts off by creating a a predefined number of particles (M) following a specific radius distribution. The number of Pt molecules in each particle is calculated using the radius. Then, the iterative process starts, the reaction speeds are calculated based on the particle radius and the PtO coverage. Then it is determined how the different reactions influence each particle. The number of Pt (n) and PtO (m) molecules in particle i at time step j can be calculated with (4) and (5). The radii of the particles are updated based

on their respective number of Pt molecules. θ is calculated for every particle. Then the process starts over with calculating the reaction speeds based on the new radius and θ. When the simulation end time is reached, the ECSA can be calculated by taking the sum of the surface of the particles.

$$n_{i,j} = n_{i,j-1} + \Delta t(-v_1(r_{i,j}) - v_2(n_{i,j}) + v_4(r_{i,j})) \quad (4)$$

$$m_{i,j} = m_{i,j-1} + \Delta t(v_2(r_{i,j}) - v_3(n_{i,j})) \quad (5)$$

Where Δt is the time step, v_{1-3} are the reactions speeds of reactions (1),(2) and (3); r is the radius of the particle.

The velocity of the electrochemical dissolution of Pt (1) can be calculated using (6).

$$v_1(r_{i,j}) = (1 - \theta_{i,j-1})k_1(r_{i,j-1}) \exp\left(\frac{F(E - E_1(r_{i,j-1}))}{2RT}\right) \quad (6)$$

Where

$$k_1(r_{i,j-1}) = k_1^{\infty}\exp\left(\frac{\beta\gamma V_{\mathrm{Pt}}}{RTr_{i,j-1}}\right) \quad (7)$$

$$E_1(r_{i,j-1}) = E_1^{\infty} - \frac{2\beta\gamma V_{\mathrm{Pt}}}{Fr_{i,j-1}} \quad (8)$$

where θ is the fraction of the particle surface that is covered by PtO; k_1 is the reaction rate constant of (1); F is the Faraday constant (96,485 C mol^{-1}); E is the electricl potential of the fuel cell; E_1 is the equilibrium potential of (1), which can be calculated using (8); R is the ideal gas constant (8.314 J mol^{-1}K^{-1}); T is the temperature of the fuel cell; k_1^{∞} is the equilibrium rate of (1) for bulk Pt (tuning parameter); β is a proportional constant between 0 and 1; γ is the interfacial surface tension ($\beta\gamma$ = j m^{-2} [19]); V_{Pt} is the molar volume of Pt (9.09e-6 m^{3}mol^{-1} at 20°C); E_1^{∞} is the equilibrium potential for Pt bulk (1.188V [17]).

The velocity of (2) can be calculated using (9).

$$v_2(r_{i,j}) = (1 - \theta_{i,j-1})k_2(r_{i,j-1}) \exp\left(\frac{F(E - E_2(r_{i,j-1}))}{2RT}\right) \quad (9)$$

Where

$$k_2(r_{i,j-1}) = k_2^{\infty}\exp\left(\frac{\beta\gamma V_{\mathrm{Pt}}}{RTr_{i,j-1}}\right) \quad (10)$$

$$E_2(r_{i,j-1}) = E_2^{\infty} - \frac{2\beta\gamma V_{\mathrm{Pt}}}{Fr_{i,j-1}} \quad (11)$$

where k_2 is the reaction rate constant for (2); E_2 is the equilibrium potential of (2); k_2^{∞} is the equilibrium rate constant of (2) (used as tuning parameter); E_2^{∞} is the equilibrium potential of (2) for Pt bulk (0.98V).

The velocity of (3) can be calculated using (12).

$$v_3(r_{i,j}) = \theta_{i,j-1}k_3(r_{i,j-1})\frac{c_{\mathrm{H+}}}{c_{\mathrm{H+}}^{\mathrm{ref}}} \quad (12)$$

Where

$$k_3(r_{i,j-1}) = k_3^{\infty}\exp\left(\frac{\beta\gamma V_{\mathrm{Pt}}}{RTr_{i,j-1}}\right) \quad (13)$$

where k_2 is the reaction rate constant for (3); k_3^{∞} is the equilibrium rate constant of (3) (used as tuning parameter); $c_{\mathrm{H+}}$ is the concentration of H^+; $c_{\mathrm{H+}}^{\mathrm{ref}}$ is the reference concentration of H^+ (1 Mol L^{-1}).

The velocity of the Ostwald ripening reaction can be calculated using (14). Because Ostwald transfers Pt molecules from one particles to another, the reaction speed can be positive or negative.

$$v_4(r_{i,j}) = 4\pi D_m C_{\mathrm{Pt}} l_c \left(\frac{r_{i,j-1}}{\bar{r}_j} - 1\right) \quad (14)$$

D_m is the diffusion coefficient for Pt (used as tuning parameter); C_{Pt} is the solubility of Pt (10^{-6} Mol L^{-1} [20]); l_c is the capillary length, taken as 1 nm [21]; $\bar{r}_j$ is the average particle radius at time step j.

Several (tuning) parameters need to be chosen to use the steady state model, see Table 1. They are picked based on a verification experiment referenced by Ao et al. [18]. The initial particle radius distribution (PRD) is taken from the same source, a lognormal distribution with $\mu = -20.5$ m and $\sigma = 0.42$ m. Additionally, the value for $c_{\mathrm{H+}}$ based on pH measurements from Healy et al. [22].

The most important information from the steady state degradation model can be found in Figure 1. The different ECSA degradation curves associated with different fuel cell voltages. It can be seen that increasing the voltage accelerates the catalyst decay.

Parameter	Value
k_1	$3 * 10^{-4}$ s^{-1}
k_2	$2 * 10^{-5}$ s^{-1}
k_3	$4 * 10^{-2}$ s^{-1}
D_m	10^3 L mol^{-1} s^{-1}
c_{H+}	10^{-4} mol L^{-1}

Table 1. Steady state degradation model Parameters

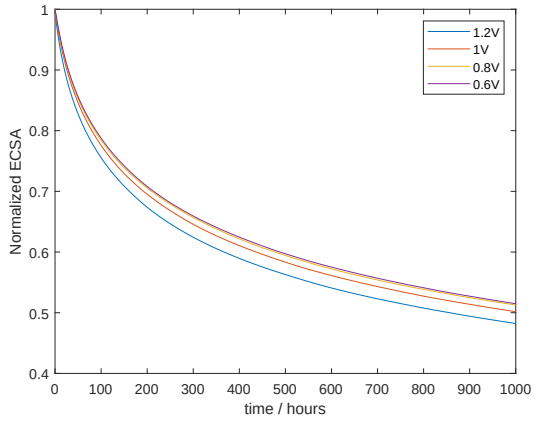

Figure 1. Steady state degradation for different FC voltages

C. Ripple degradation model

Because the (catalyst) degradation mechanisms associated with current ripple are still unclear, the ripple degradation model is based on experimental data. To extrapolate the experimental data to other ripple shapes, the electrical behaviour of the fuel cell needs to be modeled, this is done following the method outlined by Fontes et al. [12]. This model will be used to predict the voltage response of the fuel cell to the current ripple.

The theoretical maximum potential of a fuel cell can be calculated using the Nernst equation, (15).

$$E_{th} = E^0 + \frac{RT}{2F} \ln\left(P_{H_2} * \sqrt{P_{O_2}}\right) \tag{15}$$

Where E^0 is the standard potential for the fuel cell reactions at a pressure of 1 bar; R is the ideal gas constant; F is the Faraday constant; T is the fuel cell temperature; P_{H_2} is the partial pressure of hydrogen and P_{O_2} is the partial pressure of oxygen.

The fuel cell voltage lowered by the activation losses, ohmic losses and transport losses, (16).

$$V_{\text{cell}} = E_{th} - \Delta V_{\text{activation}} - \Delta V_{\text{ohm}} - \left|\Delta V_{\text{transport}}\right| \tag{16}$$

The Tafel equation (17) returns the activation overvoltage as a function of the current (I). The α represents the charge transfer coefficient. I_0 is the exchange current density, a measure of the activity at the electrode surface.

$$\Delta V_{\text{activation}} = \frac{RT}{2\alpha F} \ln\left(\frac{I}{I_0}\right) \tag{17}$$

The transport losses can be calculated using (18).

$$\Delta V_{\text{transport}} = \frac{RT}{2\beta_* F} \ln\left(1 - \frac{I}{I_{\text{lim}}}\right) \tag{18}$$

Where β_* is a tuning parameter and I_{lim} is the maximum current. The maximum current density is assumed to be 2 $A.cm^{-2}$, the fuel cell surface area is 200cm^2, giving a limit of 400 A.

The conduction losses are modeled using the membrane resistance R_{mem}, as in (19).

$$R_{\text{mem}} = \frac{l}{\sigma S} \tag{19}$$

Where l is the thickness of the membrane in cm (0.02 cm), and S is the fuel cell area in cm^2 (200 cm^2).

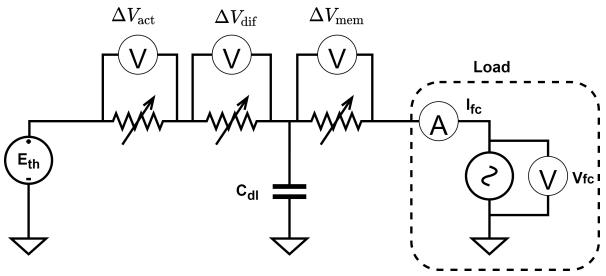

Figure 2. Fuel cell impedance model circuit. The polarizations are modeled as variable resistors.

Parameter	Value
α	0.34
I_0	0.001 A
β	0.26
I_{lim}	400 A
λ_{m}	38.8
C_{dl}	10 F

Table 2. Ripple degradation model parameters

σ is the conductivity of the membrane, Mennola [23] gives (20) to calculate it.

$$\sigma = (0.005139\lambda_m - 0.00326)* \exp\left(1268\left(\frac{1}{300} - \frac{1}{T}\right)\right) \quad (20)$$

Which calculates the conductivity using the hydration level λ_m and the temperature.

The electrical behaviour of the fuel cell is modeled using the equivalent electrical circuit shown in Figure 2. The polarizations are converted to variable resistances that change based on the current and temperature.

The parameters used in the previous equations are based on two experimental characterizations of the fuel cell, the polarization curve and an EIS. The membrane resistance is obtained using the EIS, it is the high frequency resistance. The EIS of a stack of five fuel cells can be found in Figure 3. When the left side of the EIS curves are extrapolated, a membrane resistance of 250 mΩis found. Using (20) and (19), a membrane hydration level (λ_{m}) of 38.8 is calculated. The double layer capacitance (C_{dl}) can also be found using the EIS data, by estimating the 'knee' of the curve and using (21). The activation resistance is the distance between the two intersections of EIS curve with the horizontal axis. An activation resistance of 1.14mΩleads to a capacitance of 10F.

$$C_{dl} = \frac{1}{2\pi f_{\text{knee}} R_{\text{act}}} \quad (21)$$

The other model parameters are estimated by using a least squares optimization method to minimize the difference between the voltages that are calculated

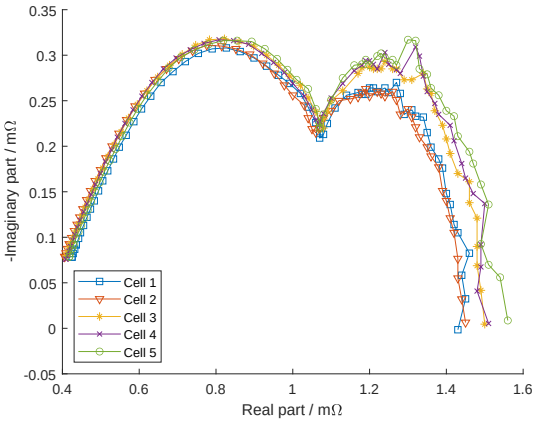

Figure 3. EIS of the five fuel cells

with (16) and the polarization curve. The polarization curve can be seen in Figure 4, the experiment was performed with a fuel cell temperature of 63°C, $P_{H_2} = 1$ bar and $P_{O_2} = 0.21$ bar. The model parameters are summed up in Table 2.

The model calculates the voltage response to the current ripple. The current ripple frequency has a significant influence on the resulting voltage ripple amplitude due to the double layer capacitance. This can be seen in Figure 5, where the voltage response to current ripples of 125±75A with 1Hz, 100Hz (low frequency current ripple) and 10,000Hz (high frequency current ripple) are compared. A high ripple frequency leads to a lower voltage ripple amplitude.

The voltage ripple amplitude is converted to the relative ECSA degradation rate by multiplying it with a base ECSA degradation rate, as shown in (22). The base ECSA degradation rate needs to be obtained using experiments.

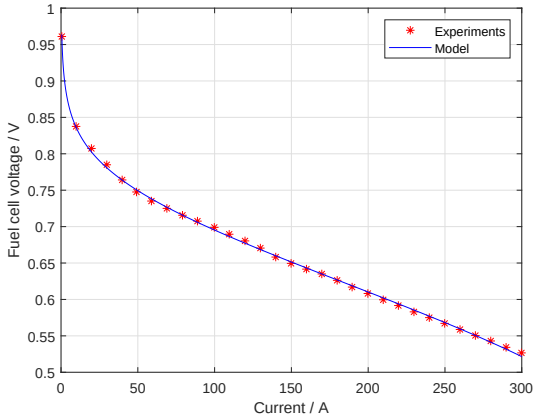

Figure 4. Fuel cell experimental and modeled polarization curves.

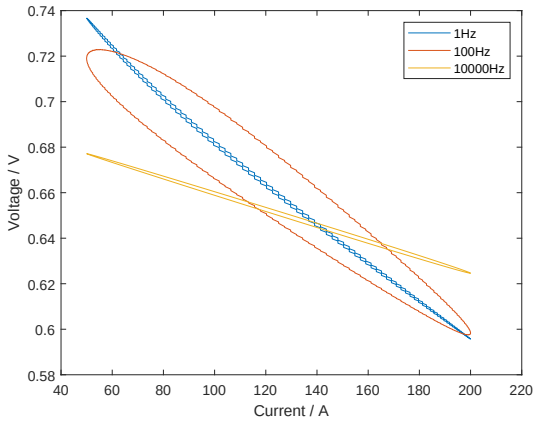

Figure 5. Voltage response to current ripples with different frequencies.

$$\text{ECSA degradation rate} = \Delta V_{\text{ripple}} * \text{base ECSA degradation rate} \quad (22)$$

But there is a lack of experimental data regarding ECSA damage due to current ripple. To illustrate the ripple degradation model EIS data is used. Kim et al. [16] report an increase of the activation resistance of 4 mΩafter 100h of being subjected to a 100Hz current ripple (0.1V peak-to-peak voltage response). This gives a base ECSA degradation rate of 0.049 $V^{-1}h^{-1}$.

III. Results

Using the placeholder base ECSA rate, a scenario can be set up to illustrate the operation of the model. The hypothetical case is a current ripple of 20% with an average current of 100A and a frequency of 20kHz. This could be caused by a boost converter. These parameters are fed into the ripple degradation model, which returns an ECSA degradation rate of $686 * 10^{-6}$ h^{-1} and an average voltage of 0.7V, which is fed into the steady state degradation model. The degradation results are visualized in Figure 6. The end of life criterion for fuel cells is often chosen as a voltage drop of 10%, this equates to a drop to 18% of the original ECSA when only considering catalyst degradation [24].

This type of data could be very useful in the design process of fuel cell systems. The lifetime of a fuel cell is an important consideration in most fuel cell applications. This can quantify the influence of the different power electronics design options (related to current ripple) on the lifetime of the catalyst.

IV. Discussion & Conclusion

Durability is one of the challenges that remain before widespread adoption of PEMFC can be reached. In this paper, a model to predict the ECSA degradation due to current ripple is introduced. The model consists of two sub-models, the steady state degradation model and the ripple degradation model, to investigate the different characteristics of current ripple that damage the catalyst.

The steady state degradation model predicts the damage due to the average current of the ripple signal,

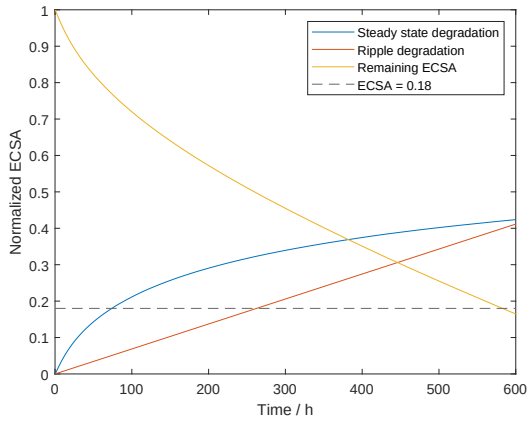

Figure 6. ECSA degradation for 20% ripple at 100A. The contributions of steady state and ripple degradation are shown. The dashed line represents the End of Live criterium.

taking into consideration the electrochemical dissolution of Pt , the chemical dissolution of Pt and Ostwald ripening, under the influence of the fuel cell potential and temperature.

The ripple degradation model calculates the ECSA loss rate based on the amplitude and frequency of the current ripple. This sub-model is built using an electrical representation of the fuel cell, combined with experimental data.

The relative contribution of the ripple degradation to the overall degradation is still unknown, however, it should be taken into account when designing fuel cell systems.

The model can be used to help in the design process of power electronics that interface with fuel cells by quantifying the impact of the produced current ripple.

Experimental verification of the model would be the next step towards a better understanding of the influence of current ripple on fuel cells.

References

[1] EU, F., "The JIVE projects celebrate a milestone 200 buses have been ordered!.pdf," , Sep. 2020. URL https://www.fuelcellbuses.eu/sites/default/files/documents/The%20JIVE%20projects%20celebrate%20a%20milestone%20200%20buses%20have%20been%20ordered%21.pdf.

[2] "Nemo H2: rondvaart op waterstof," , Jul. 2011. URL https://www.rvo.nl/sites/default/files/rvo_website_content/EOS/DEMO06005.pdf.

[3] partnership, U. D., "Fuel Cell Technical Team Roadmap," , 2017. URL https://www.energy.gov/sites/default/files/2017/11/f46/FCTT_Roadmap_Nov_2017_FINAL.pdf.

[4] De Bruijn, F., Dam, V., and Janssen, G., "Durability and degradation issues of PEM fuel cell components," *Fuel cells*, Vol. 8, No. 1, 2008, pp. 3–22. Publisher: Wiley Online Library.

[5] Jahnke, T., Futter, G., Latz, A., Malkow, T., Papakonstantinou, G., Tsotridis, G., Schott, P., Gérard, M., Quinaud, M., Quiroga, M., and others, "Performance and degradation of Proton Exchange Membrane Fuel Cells: State of the art in modeling from atomistic to system scale," *Journal of Power Sources*, Vol. 304, 2016, pp. 207–233. Publisher: Elsevier.

[6] Shao-Horn, Y., Sheng, W., Chen, S., Ferreira, P. J., Holby, E., and Morgan, D., "Instability of supported platinum nanoparticles in low-temperature fuel cells," *Topics in Catalysis*, Vol. 46, No. 3, 2007, pp. 285–305. Publisher: Springer.

[7] Restrepo, C., Konjedic, T., Calvente, J., and Giral, R., "A review of the main power electronics advances in order to ensure efficient operation and durability of PEMFCs," *Automatika: asopis za automatiku, mjerenje, elektroniku, raunarstvo i komunikacije*, Vol. 53, No. 2, 2012, pp. 184–198.

[8] Thounthong, P., Sethakul, P., Rael, S., and Davat, B., "Fuel cell current ripple mitigation by interleaved technique for high power applications," *2009 IEEE Industry Applications Society Annual Meeting*, IEEE, 2009, pp. 1–8.

[9] Gemmen, R. S., "Analysis for the effect of inverter ripple current on fuel cell operating condition," *J. Fluids Eng.*, Vol. 125, No. 3, 2003, pp. 576–585.

[10] Choi, W., "New approaches to improve the performance of the PEM based fuel cell power systems," PhD Thesis, Texas A&M University, 2005.

[11] Zhan, Y., Guo, Y., Zhu, J., Liang, B., and Yang, B., "Comprehensive influences measurement and analysis of power converter low frequency current ripple on PEM fuel cell," *International Journal of Hydrogen Energy*, Vol. 44, No. 59, 2019, pp. 31352–31359. Publisher: Elsevier.

[12] Fontes, G., Turpin, C., Astier, S., and Meynard, T. A., "Interactions between fuel cells and power converters: Influence of current harmonics on a fuel cell stack," *IEEE Transactions on Power Electronics*, Vol. 22, No. 2, 2007, pp. 670–678. Publisher: IEEE.

[13] Gerard, M., Poirot-Crouvezier, J.-P., Hissel, D., and Pera, M.-C., "Ripple current effects on PEMFC ag-

ing test by experimental and modeling," *Journal of fuel cell science and technology*, Vol. 8, No. 2, 2011. Publisher: American Society of Mechanical Engineers Digital Collection.

[14] Kim, J.-H., Jang, M.-H., Choe, J.-S., Kim, D.-Y., Tak, Y.-S., and Cho, B.-H., "An experimental analysis of the ripple current applied variable frequency characteristic in a polymer electrolyte membrane fuel cell," *Journal of Power Electronics*, Vol. 11, No. 1, 2011, pp. 82–89.

[15] Wahdame, B., Girardot, L., Hissel, D., Harel, F., François, X., Candusso, D., Pera, M. C., and Dumercy, L., "Impact of power converter current ripple on the durability of a fuel cell stack," *2008 IEEE International Symposium on Industrial Electronics*, IEEE, 2008, pp. 1495–1500.

[16] Kim, J., Lee, I., Tak, Y., and Cho, B., "Impedance-based diagnosis of polymer electrolyte membrane fuel cell failures associated with a low frequency ripple current," *Renewable energy*, Vol. 51, 2013, pp. 302–309. Publisher: Elsevier.

[17] Cherevko, S., Kulyk, N., and Mayrhofer, K. J., "Durability of platinum-based fuel cell electrocatalysts: Dissolution of bulk and nanoscale platinum," *Nano energy*, Vol. 29, 2016, pp. 275–298. Publisher: Elsevier.

[18] Ao, Y., Chen, K., Laghrouche, S., and Depernet, D., "Proton exchange membrane fuel cell degradation model based on catalyst transformation theory," *Fuel Cells*, 2021. Publisher: Wiley Online Library.

[19] Vengrenovitch, R., "On the Ostwald ripening theory," *Acta metallurgica*, Vol. 30, No. 6, 1982, pp. 1079–1086. Publisher: Elsevier.

[20] Jinnouchi, R., Toyoda, E., Hatanaka, T., and Morimoto, Y., "First principles calculations on site-dependent dissolution potentials of supported and unsupported Pt particles," *The Journal of Physical Chemistry C*, Vol. 114, No. 41, 2010, pp. 17557–17568. Publisher: ACS Publications.

[21] De Smet, Y., Deriemaeker, L., and Finsy, R., "A simple computer simulation of Ostwald ripening," *Langmuir*, Vol. 13, No. 26, 1997, pp. 6884–6888. Publisher: ACS Publications.

[22] Healy, J., Hayden, C., Xie, T., Olson, K., Waldo, R., Brundage, M., Gasteiger, H., and Abbott, J., "Aspects of the chemical degradation of PFSA ionomers used in PEM fuel cells," *Fuel cells*, Vol. 5, No. 2, 2005, pp. 302–308. Publisher: Wiley Online Library.

[23] Mennola, T., "Design and experimental characterization of polymer electrolyte membrane fuel cells," 2000, p. 92.

[24] Wang, Y., Moura, S. J., Advani, S. G., and Prasad, A. K., "Power management system for a fuel cell/battery hybrid vehicle incorporating fuel cell and battery degradation," *International Journal of Hydrogen Energy*, Vol. 44, No. 16, 2019, pp. 8479–8492. Publisher: Elsevier.